UNIVERSIDADE DE LISBOA
FACULDADE DE CIÊNCIAS
DEPARTAMENTO DE ENGENHARIA GEOGRÁFICA, GEOFÍSICA E ENERGIA

Characterization of particulate emissions from biomass power plants

João Luís Siopa da Silva

Dissertação de Mestrado

Mestrado Integrado em Engenharia da Energia e do Ambiente

2015

UNIVERSIDADE DE LISBOA
FACULDADE DE CIÊNCIAS
DEPARTAMENTO DE ENGENHARIA GEOGRÁFICA, GEOFÍSICA E ENERGIA

Characterization of particulate emissions from biomass power plants

João Luís Siopa da Silva

Dissertação de Mestrado orientada pela:

Professora Doutora Helena Lopes (FCUL/LNEG)

Doutora Ana Teresa Crujeira (LNEG)

Mestrado Integrado em Engenharia da Energia e do Ambiente

2015

Master dissertation developed in the scope of Project FCOMP-01-0124-FEDER-019346 – BiomAshTech *Impactos da Cinza na Conversão Termoquímica de Biomassa*, financed by FEDER Competitiveness Factors Thematic Operational Program – COMPETE and National support through FCT – Fundação para a Ciência e a Tecnologia.

DEDICATION

To professor Dr. Helena Lopes for the great and fulfilling opportunity that was this project, I truly appreciate it. For the availability and dedication during this period, the long and very educational conversations and the very effective work methods.

To Dr. Ana Teresa Crujeira for the warm welcome to the project and for the companionship during the physically-demanding sampling work. For the support and the vast knowledge transmission, that helped the writing of this thesis.

To Dr. Fernanda Guimarães for the great and much useful work with the SEM equipment, at LNEG's S. Mamede de Infesta Campus. To Dr. Teresa Diamantino for allowing the use of the stereo microscope equipment and to Dr. Teresa Ferraz for the technical support and enthusiasm during the observations.

To Dr. Luis Tarelho for the technical support during the sampling period. To Dr. Paula Teixeira and Márcia Freire M. Sc. for the availability and good will in helping with any task. To David Salema M. Sc. for the technical support with the TESTO analyser and with its data interpretation, and also the productive technical discussions.

To Dr. Ascensão Trancoso for the interesting conversations, suggestions, support and enthusiasm.

To my dear friends from MIEEA 2008, this was an amazing adventure and the best part was having you around.

To my much loved friends Carolina, Joana, José, Liliana, Manuela, Mónica, Rafael, Raisa and Ricardo. I can only be grateful for having you in my life. Thank you, always.

To my parents, Bentes and Belinha, the unconditional supporters in everything I choose in my life; my grandparents, Fonseca and Cândida, my greatest inspiration and the legacy I stand for and; my brother Pedro for everything you taught me.

A special dedication to my grandfather, Avô Fonseca.

ACKNOWLEDGMENTS & FRAMEWORK

BiomAshTech is a project headed by University of Aveiro, Portugal, with participation of LNEG – Laboratório Nacional de Energia e Geologia, with Helena Lopes PhD as principal Investigator. The project focuses on the study of the inorganic material behaviour from various types of national biomass, in order to control the pollutant emissions and formation of problematic ashes in combustion systems.

This subject selection for my Master's Dissertation came from my increasing interest in the areas of the combustion technologies and biomass and waste energy. Interest that was developed during my academic course in Lisbon (FCUL) and in Germany (FH Aachen), during an Erasmus year, and also as an intern at the Electricity Museum in Lisbon. The opportunity to work at an industrial unit was also crucial on my decision.

The present document is the result of the work developed during an internship at LNEG, in order to achieve the Master Degree in Environmental and Energy Engineering from Faculty of Sciences of University of Lisbon – FCUL. The internship was held under the supervision of Professor Helena Lopes PhD (FCUL/LNEG) and Ana Teresa Crujeira PhD (LNEG).

The objective of this internship focused on characterization of emitted particles in the flue gas from an Industrial biomass-fired power plant, with later chemical and morphologic analyses of the samples. Pollutant emissions during combustion were also studied.

The activities developed can be summarized in:

1. Bibliographic research on particles emissions from biomass-fired combustion systems
2. Training in stationary source emissions sampling;
3. Training in particle chemical and morphological characterization;
4. Particle sampling at an Industrial unit stack's external platform;
5. Particle samples chemical and morphological characterization;
6. Theoretical determinations of excess air and fuel, stoichiometric air and gases emission flow.

ABSTRACT

The efforts for energy sector decarbonisation led to the increase of biomass consumption, considered as a low GHG emissions fuel. Besides the low carbon emissions, also NO_x and SO_2 emissions can be reduced in fluidized bed (FB) combustion system, respectively, *ca* 83 % and 90 % of reduction can be achieved. This happens due to the biomasses composition and the FB systems characteristics, therefore the biomass-fired PP only need a fly-ash/particle removal system, usually an electrostatic precipitator (ESP).

The bio-advantage of the biomass as fuel is confronted if some drawbacks, such as the high water and inorganic (ashes) content. Also, the possible presence of significant chlorine content from the fuel may result in relevant HCl emissions, possibly raising the need for an ELV legislation to control Cl base pollutants from biomass combustion systems.

The present work focused on the emitted particulate matter, particulate size distribution, constitution and morphology at a Portuguese medium combustion biomass-fired plant (between 20 MW_{th} and 50 MW_{th}). The methods used were: Total Suspended Particulate (EN 13284-1:2009), Particulate Granulometric Classification (*Mark III user's manual*, based on the U.S. EPA Method 5) and $PM_{10/2,5}$ (EN ISO 23210:2009). Particles collected were observed using Microprobe/SEM for morphology and composition.

Finer particles, with aerodynamic diameters below 10 µm, presented chlorine (Cl) and also a high alkali content, namely of Calcium (Ca), Potassium (K) and Sodium (Na), with fuel's origin, as well as Silica (Si), a consequence of soil and stone contamination in addition to fuel's origin and sand from the fluidized bed system. For the submicron (ranges below 0,43 µm) lead (Pb), a highly toxic heavy metal for the human health, was detected in discrete forms, despite the low amounts usually present in the biomass used in the power plant.

KEY WORDS: Biomass Combustion; Combustion pollutants; Particulate matter emission; $PM_{10/2,5}$

RESUMO

Os esforços para a descarbonização do sector energético levaram a aumento do consumo de biomassa, considerado um combustível com baixas emissões de gases com efeito de estufa. Para além das baixas emissões de carbono, também as emissões de NO_x e SO_2 podem ser reduzidas em sistemas combustão de leito fluidizado (LF), respetivamente, *ca* 83 % e 90 % de redução podem ser atingidos. Facto relacionado com a composição das biomassas e com as características do sistema LF, assim, as centrais a biomassa apenas necessitam de sistemas para remoção de partículas, normalmente percipitadores electroestáticos (ESP).

A bio-vantagem da biomassa como combustível é confrontada com alguns problemas como o alto conteúdo em água e o conteúdo inorgânico (cinzas). Também, a possível presença significativa de cloro do combustível pode resultar em emissões de HCl relevantes, possivelmente levando à necessidade de criação de legislação, valores de emissões limite, para controlar poluentes com origem em Cl nos sistemas de combustão a biomassa.

O presente trabalho focou-se no material particulado emitido, a distribuição de diâmetros das partículas, a consituiçao e morfologia numa central portuguesa de média dimensão a biomassa (entre 20 MW_{th} e 50 MW_{th}). Os métodos utilizados foram: Partículas Totais em Suspensão (EN 13284-1:2009), Classificação Granulométrica de Partículas (Manual de utilizador do *Mark III*, baseado no Método 5 da EPA) e $PM_{10/2,5}$ (EN ISO 23210:2009). As partículas coletadas foram observadas utilizando microssonda/SEM para morfologia e composição.

Partículas finas, com diâmetros aerodinâmicos inferiores a 10 µm, apresentaram Cl e também um alto conteúdo alcalino, nomeadamente de Cálcio (Ca), Potássio (K) e Sódio (Na), com origem no combustível, bem como Sílica (Si), uma consequência de contaminação por solo e rochas, em adição à origem do combustível e areia do sistema LF. Para a partículas submicrónicas (inferiores a 0,43 µm) Chumbo (Pb), um metal pesado altamente tóxico para a saúde humana, foi detetado de forma discreta, apesar das pequenas quantidades normalmente apresentada na biomassa usada na central.

PALAVRAS-CHAVE: Combustão de biomassa; Poluentes da combustão; Emissão de material particulado; $PM_{10/2,5}$.

Contents

ABBREVIATIONS & SYMBOLS

acfm	Actual cubic feet per minute
BAT	Best Available Technology
BFB	Bubbling Fluidized Bed
CAFE	Ambient air quality and Cleaner Air For Europe
CEMS	Continuous Emission Monitoring System
CFB	Circulating Fluidized Bed
CHP	Combined Heat and Power
d.b.	Dry basis
D-ESP	Dry Electrostatic Precipitator
EPA	U.S. Environmental Protection Agency
ESP	Electrostatic Precipitator
FB	Fluidized Bed
FIT	Feed-In Tariff
GHG	Green House Gases
IED	Industrial Emissions Directive
IPPC	Integrated Pollution Prevention and Control
LCP	Large Combustion Plant Directive
LHV	Low Heating Value
LRTAP	Long Range Transboundary Air Pollution
MCP	Medium Combustion Plant Directive
NDIR	Non-dispersive infrared
Nm^3	Volume at standard conditions for temperature and pressure
NREAP	National Renewable Energy Action Plan
OECD	Organisation for Economic Co-operation and Development
PCCD/F	Dioxins/Furans
PGC	Particulate Granulometric Classification
PM	Particulate Matter
PM10/2,5	Particulate Matter with 10 µm and 2,5 µm aerodynamic diameter
PP	Power Plant
SEM	Scanning Electron Microscopy
TSP	Total Suspended Particles
SRC	Selective Catalytic Reduction
vol%	Volume percentage
W-ESP	Wet Electrostatic Precipitator
w.b.	Wet basis
WID	Waste Incineration Directive
wt%	Weight percentage

$A; A_s$ – Cross-sectional area of stack (m^2)

A_n – Cross-sectional area of nozzle (m^2)

C (129 m/s (kg/kmol K)$^{1/2}$)

C_{avg} – average concentration during sampling period (mg/Nm^3)

$C_{chlorides(HCl)}$ – Mass concentration of gaseous chlorides at standard conditions of temperature and pressure (mg/Nm^3)

C_{ref} – Reference oxygen content concentration (mg/Nm^3)

c_s – Particles concentration (mg/Nm^3)

I – Isokinetic sampling (%)

$K; C_p$ – Type S Pitot tube coefficient, dimensionless (0,85)

K_4 (0,003454 (mmHg m^3)/(mL K))

K_p –Velocity equation constant (method 2) (34,97 m/s[(g/mol)(mm Hg)]/[(K)(mm H_2O)]$^{1/2}$)

K_{HCl} – 1,028 ((µg HCl/µg-mole)/(µg Cl -/µg-mol))

M_d – Molecular weight of stack gas, dry basis (g/g-mol)

M_{HCl} – Molecular weight of HCl (36,46 g/g-mol)

M_{Cl} - Molecular weight of Cl (35,45 g/g-mol)

M_s – Molecular weight of stack gas, wet basis (g/g-mol)

M_W – Molecular weight of water (18,0 g/g-mol)

$m_{chlorides}$ – Mas concentration of gaseous chlorides collected in the sample absorption solution (mg)

m_p – Particles mass (mg)

m_{wc} – Mass of water vapour collected in the trapping unit (g)

$O_{2\ ref}$ – reference oxygen content (%)

$O_{2\ avg}$ – average reference oxygen content (%)

P_{bar} – Barometric pressure at measurement site (mmHg)

P_g –Stack static pressure (mmHg)

$p_e; P_s$ – Absolute stack pressure, $P_{bar} + P_g$ (kPa; mmHg)

p_{std}; P_{std} – Standard absolute pressure (101,3 kPa; 760 mmHg)

Q_s – Particles mass flow (kg/h)

$q_{vr}; Q_{sd}$ – Dry volumetric stack gas flow rate corrected to standard conditions (m^3/s; m^3/h)

R – Ideal gas constant (0,06236 (mmHg m^3)/(g-mol K))

T_m – Absolute temperature at meter (K)

T_s –Stack temperature (K)

T_{std} – Standard absolute temperature (273,15 K)

$V_m; (V_2 - V_1)$ – Dry gas volume measured by dry gas meter (m^3, dcm)

$V_{m(std)}$ – Dry gas volume measured by the dry gas meter, in standard conditions (m^3, dscm)

$V_{mol(std)}$ - Molar volume at standard conditions (22,4x10^{-3} m^3/mol at p_{std} and T_{std})

$V_{w(std)}$ – Volume of water vapour condensed, corrected to standard conditions (m^3, scm)

$V_{wc(g/m3)}$ – Water vapour content on dry basis (g/m^3)

$V_{wc(\%)}$; B_{ws} – Water vapour in the gas stream (%)

$\bar{v}$; v_s – Average stack gas velocity (m/s)

v_a – Velocity of the gas entering the sampling nozzle (m/s)

v_N – Velocity of the in the duct at the sampling point (m/s)

Y – Dry gas meter calibration factor (1)

ΔH – Samples gas pressure differential across the orifice (mmH$_2$O)

Δp; ΔP – Pressure differential across the S-type pitot tube (mmH$_2$O)

θ - Sampling time (min)

ρ_w – Density of water (0,9982 g/mL)

$\%e_{air}$ – Excess Air

LIST OF FIGURES

LIST OF TABLES

1 INTRODUCTION

Emissions of greenhouse gases have been a major worldwide concern due to increasing population and consequent increasing of industries and energy consumption so satisfy its needs. The energy sector is considered to be the largest source of carbon dioxide into the atmosphere, due to use of fossil fuels in transportation, heat and power generation for a wide range of industrial processes (pulp and paper, concrete industries among other). Therefore, major concerns regarding energy efficiency, sustainability and renewable energy have been increasing, straightening the energy area with the environmental science.

The European Union has been a great supporter of renewable energies, through strategic energy plans and policies, and established concrete targets for exploitation of indigenous renewable energy sources, and for bioenergy in particular. The 2020 climate and energy package, also known as the Packet 20-20-20, from 2008, aims for a 20 % reduction in EU greenhouse gas emissions from 1990 levels, raising the share of EU energy consumption produced from renewable resources to 20 % and a 20 % improvement in the EU's energy efficiency (EC, 2015).

Committed to reducing greenhouse gas emissions from 80 % to 95% below 1990 levels by 2050, the EU is exploring new challenges of decarbonisation, based on the Energy Roadmap 2050 (EC, 2011) . Among the proposed solutions is the decrease of coal share in energy production using co-firing with biomass.

Biomass is as a good alternative energy supplier, mainly because its net CO_2 emissions are much less than those of fossil fuels. It is a versatile fuel, being used for power and heat generation and also to produce biofuels for the transportation sector. It is also an indigenous renewable energy source, with great storage advantages.

These reasons are making biomass combustion more and more attractive. However, the adverse health effects of fine particles, among other drawbacks, have become an important issue and fine particle emissions from biomass combustion are considered to be one of the major sources. The inorganic content of biomass present a great problem for combustion systems, which leads to important research area, with the aim to achieve good environmental performance of solid biofuels utilization for energy, since the new plant construction and the conversions of coal-fired power plants will one of the main solid biomass energy development priority for the years to come (EurObserv'ER, 2013).

1.1 BIOMASS TO ENERGY

The Directive on the promotion of the use of energy from renewable sources (Directive 2009/28/EC) define Biomass as the biodegradable fraction of products, waste and residues from biological origin from agriculture (including vegetal and animal substances), forestry and related industries, fisheries and aquaculture, as well as the biodegradable fraction of industrial and municipal waste.

In industrialized countries biomass contributes, on average, from 9 % to 14 % of the total energy supply, but in developing countries this can get as high as one-fifth to one-third, due to domestic uses such as cooking and heating (Khan *et al.*, 2009).

As a fuel, biomass is used in a wide range of applications: small-scale stoves, large-scale boilers, large heating plants, etc. It is also used in cogeneration plants to produce both electricity and heat – Combined Heat and Power (CHP) plant – with average efficiency from 75 % to 90 % (BAT, 2006). Combustion is the most important and mature technology available for biomass utilization, either for heat or electricity production (Nussbaumer, 2003).

According to OECD (1991), “CO_2 emissions resulting from bioenergy consumption should not be included in a country’s official emission inventory”, considering that the biomass converted into energy consumed CO_2 during its life. This is still the most commonly used approach for bioenergy systems life cycle assessments, although nowadays other approaches, considering greenhouse gases emissions have been discussed (Cherubini *et al.*, 2011).

1.1.1 SECTOR CHARACTERIZATION

The European continent counted a wood supply of around 24 144 million m^3 in 2008 (Alakangas *et al.*, 2012). The largest flows of wood are used in mechanical, semi-mechanical and chemical pulp industry, sawn timber and fibre and particle board industry. In each of these industries there is a large share in energetic use of wood, used as solid biofuel or black liquor.

In the scope of the renewable sources promotion in a new energy policy, in 2005 the European Union (EU) presented the Biomass Action Plan (EC, 2005). When the plan was released, biomass met 4 % of the EU's energy needs – 69 Mtoe – and the aim was to increase its use to around 150 Mtoe by 2010.

The Directive 2009/28/EC on the promotion of the use of energy from renewable sources stablishes the target of, at least, 20 % for the share of energy from renewable sources in the gross final consumption of energy in the year 2020. Each member state should adopt a national renewable energy action plan in order to meet these targets. This target is in line with the overall Target 20-20-20 for the EU.

Solid and gaseous biomass used for electricity, heating and cooling production constitutes the biggest source of renewable energy in the EU. According to estimates from the National Renewable Energy Action Plan (NREAP), it is expected to further increase from 86,5 Mtoe in 2012 up to 110,5 Mtoe in 2020.

Solid biomass use for heat and electricity production has increased at an annual rate of 3,8 % since the year 2000 rising to a total of 82,3 Mtoe by 2012. The bioelectricity output reached 79,5 TWh in 2012, with 26,5 TWh coming from PP only and 53,1 TWh from CHP plants (EurObserv'ER, 2013).

Wide-scale expansion of bioelectricity production and cogeneration, through new plant construction or the conversion of coal-fired PPs, will be the main solid biomass energy development priority for the years to come.

Focusing on the Portuguese territory, 38 % is covered by forest, presenting an available forest biomass potential of around 2,2 million ton/year (Marques, 2013). Portugal is a country where the wood, cork, paper industry and agricultural activities have a major role in the economy. From these industries a great amount of residues are obtain from the various production steps.

The energy policy stated by the Energetic National Strategy of 2005 (*Plano Nacional para a Energia – RCM nº 169/2005*), aims to enhance the environmental performance in energy laws. On the biomass valorisation chapter, the objective was to increase the power capacity as well as to adopt new forestry biomass valorisation measures, cooperating with the wood and the paper & pulp industries. In order to increase the power capacity, in 2006 a project to build fifteen new forestry biomass PPs with a total power of 100 MW until 2010 was planned. To prompt this plan a favourable feed-in tariff (FIT) was established, around 109 €/MWh, for the energy generated in forest biomass PPs.

The plan was unsuccessful, with only two of the biomass PP built (*Termoeléctrica de Belmonte* and *Termoeléctrica da PALSER*). Some of the appointed reasons for the failure were bad PP's location, high resource price (when analysed against the available tariff), resource supply issues, logistics and availability in the process.

However, externally to this plan, between 2007 and 2009, five new biomass PP with a total capacity of 78 MW were built in Portugal. By 2011 the FIT for forest biomass was set to be 119 €/MWh. The FIT is guaranteed for a period of 15 years, or for an amount of 33 GWh/MW capacity installed.

Existing industrial CHP and PP, using biomass as fuel, are summarized in Table 1.

***Table 1** – Biomass-fired Plants in Portugal (adapted from e2p (INEGI))*

Name	**Location (District)**	**Technology**	**Electrical Capacity (MW_e)**	**Begin of production (year)**
COSTA IBÉRICA	Viseu	CHP	0,3	2011
Cogeração Amorim	Aveiro	CHP	1,1	2004
Termoeléctrica de Belmonte*	Castelo Branco	PP	2	2010
Termoeléctrica da PALSER*	Castelo Branco	PP	3	2010
Cogeração SIAF	Viseu	CHP	4	1996
Termoeléctrica Centroliva	Castelo Branco	PP	6	1998
Cogeração Caima	Santarém	CHP	9	2001
Termoeléctrica de Mortágua	Viseu	PP	9	1999
Termoeléctrica Terras de Sta. Maria	Aveiro	PP	10	2008
Termoeléctrica de Cacia	Aveiro	PP	12,5	2009
Termoeléctrica de Setúbal	Setúbal	PP	12,5	2009
Termoeléctrica de Ródão	Castelo Branco	PP	13	2007
Termoeléctrica de Constância	Santarém	PP	13,7	2009
Cogeração Celtejo	Castelo Branco	CHP	30	1992
Termoeléctrica da Figueira da Foz	Coimbra	PP	34,3	2009
Cogeração de Cacia	Aveiro	CHP	35,1	2005
Cogeração EUROPA&C Energia Viana	Viana do Castelo	CHP	38,8	2002
Cogeração de Setúbal	Setúbal	CHP	53,9	2004

Name	Location (District)	Technology	Electrical Capacity (MW_e)	Begin of production (year)
Cogeração Celbi	Coimbra	CHP	70	1987
Cogeração da Figueira da Foz (Lavos)	Coimbra	CHP	95	2004

*from the 2006 Plan

The Portuguese target for the share of energy from all renewable sources in gross final consumption of energy should be 31 % for the year 2020 (PNAER, 2009). The projected NREAP share in that year exactly matches the target. Based on the projection, the most important contribution is expected from biomass with 2 322 ktoe (1 484 ktoe from solid biomass), accounting for 38 % of all renewable energy.

Biomass accounted 55 % of all renewable energy share in the primary energy production in Portugal in 2012 (DGEG, 2014). Also, the primary energy production of solid biomass reached 2,342 Mtoe (EurObserv'ER, 2013).

In Portugal the gross electricity production from biomass in 2013 reached 2 516 GWh, with 1 780 GWh of that production coming from CHP and 736 GWh from PP, from a total electrical capacity of around 426 MW_e (DGEG, 2014). The Portuguese NREAP aims for a total electrical capacity of 958 MW_e by 2020, with 436 MW_e coming from systems with cogeneration, to increase energy production efficiency.

The increasing demand of biomass to energy must be satisfied by a diversified set of existing biomass feedstocks not currently used because they are often considered of low quality (wastes from agricultural, agro industrial and forestry activities). However, these practices will have to be hand-to-hand with sustainable management of biomass natural resources to be used as solid biofuels.

1.1.2 SOLID BIOFUEL CHARACTERISTICS

Biomass energy resources are diverse and therefore a comprehensive classification system was created, in order to predict its behaviour by identifying to which class belongs and also establishing rules for managing and utilization. The classification can be based in the following concepts: (1) the biomass origin – primary, secondary and tertiary residues and energy crops (Williams, 1992); (2) the biomass properties – wood and woody fuel, herbaceous fuels, wastes, derives, aquatic and energy crops (Jenkins *et al.*, 1998); (3) International Standard for Solid biofuels – Fuel specifications and classes (ISO14961, 2005) – woody biomass, herbaceous biomass, fruit biomass, blend and mixtures.

Biomass composition includes cellulose, hemicelluloses, lignin, lipids, proteins, simple sugars, starches, water, hydrocarbon, ash (inorganic compounds), and other compounds. The concentration of each class of compounds varies depending on specie, type of plant tissue, stage of growth, and growing conditions. These concentrations influence the combustion performance and the characteristics related with quantity and chemical composition of the ashes produced during thermochemical conversion of biomass to energy at power plants.

Biomass offers important advantages as a combustion feedstock due to the high volatility of the fuel and the high reactivity of both the fuel and the resulting char.

The bulk composition of biomass in terms of carbon, hydrogen, and oxygen (CHO) does not differ much among different biomass sources. Typical (dry base) weight percentages for C, H, and O are 30 % to 60 %, 5 % to 6 %, and 30 % to 45 %, respectively (Jenkins *et al.*, 1998). Nitrogen, sulphur and chlorine can also be found in quantities usually less than 1%, but occasionally well above depending on the biomass type. When compared to coal, biomass presents higher share of moisture, ashes, oxygen, nitrogen, silicon, potassium; low heating value (LHV)– generally from 18 to 21 MJ/kg (dry base) – and less carbon, aluminium and iron contents.

The wood and woody materials tend to be low in nitrogen, chlorine and ash content, whereas the agricultural Biomass residues, generally herbaceous biomass, can have higher content of these components (Obernberger *et al.*, 2006).

A comparison of various wood and herbaceous biomass compositions is summarized in Table 2, presenting typical guiding values for ash, LHV and element concentrations of several biomass species.

Table 2 –Biomasses characterization, typical mean values (adapted from ISO14961 (2005))

(LHV – Low Heating Value; d.b. - dry basis; wt% - weight percentage)

Parameter	Unit	Wood biomass			Herbaceous biomass	
		Wood without bark	Bark	Logging residues	Straw	Grass
LHV	MJ/kg (d.b.)	19,1	20	20	17,8	18,1
Ash	wt% d.b.	0,3	4,0	2,0	5	7
C		51	54	51	47	47
H		6,3	6,1	6	6	6
O		42	40	40	41	41
N		0,1	0,5	0,5	0.5	1.3
S		0,02	0,1	0,04	0,1	0,2
Cl		**0,01**	**0,02**	**0,01**	**0,4**	**0,8**
F		<0,0005	0,001	-	0,0005	0,001
Al	mg/kg d.b.	100	800	-	50	200
Ca		900	5000	5000	4000	3500
Fe		25	500	-	100	600
K		400	2000	2000	10 000	15 000
Mg		150	1000	800	700	1700
Mn		147	500	251	-	-
Na		20	300	200	500	1000
P		60	400	500	1000	3000
Si		150	2000	3000	10 000	15 000
Ti		<20	-	-	-	-
As	mg/kg d.b.	<0,1	1	0,3	<0,1	0,1
Cd		0,1	0,5	0,2	0,1	0,2
Cr		1	5	-	10	1
Cu		2	5	-	2	5
Hg		0,02	0,05	0,03	0,02	<0,02
Ni		0,5	10	-	1	2
Pb		2	4	3	0,5	1
V		<2	1	-	3	3
Zn		10	100	-	10	25

Wood by-products and wood residues, from industrial production when chemically treated, with wood preservatives or coating, can raise the amount of heavy metals or halogenated organic compounds (ISO14961, 2005).

Ash contents in solid biofuels is one of the main technical challenges for combustion systems, since they may present low melting temperature and sintering tendency due to its high alkali content (especially K), together with chlorine content of biomass (Khan *et al.*, 2009). This is relevant in some woody biomass residues and herbaceous or fruit residues and may lead to problems in the systems such as: fouling, deposition, corrosion, slagging and agglomeration.

Slagging is the formation of molten or partially fused deposits on furnace walls or convection surfaces exposed to radiant heat. Fouling consists on the formation of layered deposits on convection heat surfaces such as superheater and reheaters. These deposits reduce the heat transfer and thus the efficiency of combustion units and can lead to plant shutdown for deposits removal and boiler cleaning (Lin *et al.*, 2003). Furthermore, deposits can be corrosive and may thus reduce the lifetime of the installations.

Agglomeration happens in the Fluidized Bed (FB) systems' bed, between the ashes and the material used in the bed (usually silica sand) which bond and reduce the bed's fluidization. In extreme cases this may lead to unscheduled shutdown of the system (Khan *et al.*, 2009).

Ashes are constituted by the inorganic non-combustible part of the fuel (essentially Al, Ca, Mg, K, Na, Fe) or from contamination – with soil, sand or stones. Therefore, the origin of phases in biomass ash is defined in three classes: Primary ashes are the original phases or minerals that come from natural processes, during the biomass living time. Their fibre structure contains Si and Ca, while K, P, S, Zn present as micro or macro nutrients; Secondary ashes result from the anthropogenic activity, regarding its new phase's generation by solid, liquid and gas reactions among pre-existing and newly formed compounds, during biomass combustion in the appropriate installations; Tertiary ashes result from natural processes, weathering, during transport and storage of combustion residues (Vassilev *et al.*, 2013).

Moisture content of biomass may range from 10 % to 70 %, the higher its content is, the lower its heating value. Flue gas volume produced per energy unit increases with moisture increase, requiring larger flue gas treatment equipment. Also, high moisture in solid biofuels can cause ignition and combustion instability.

In Portugal the most common type of solid biofuel used in PP are a variety of forest biomass residues from forestry related activities (Tarelho *et al.*, 2011). It consists mainly in material from eucalyptus (*Eucalyptus globulus*) and pine (*Pinus pinaster*) processing. This fuel may contain a significant amount (can be as high as 25wt%) of inertial material – soil particles and stones from the forest – mixed, which can result from bad management practices in the forest during harvesting and biomass management operations.

1.1.3 SOLID BIOFUEL COMBUSTION

Combustion is defined as the rapid chemical combination of oxygen with the combustible elements of a fuel, consisting of consecutive heterogeneous and homogenous reactions, leading to the release of heat and final products.

Biomass combustion is a complex process which depends both on the fuel properties and the combustion application. The combustion process of solid fuels can be specified into the following main stages: drying, pyrolysis/gasification and oxidation (Nussbaumer, 2003).

The drying process consists in the evapouration of the moisture present in the fuel at temperatures around 100 ˚C. This endothermic reaction, evapouration, consumes part of the energy released in the combustion process, meaning that the amount of moisture in the fuel can influence the efficiency of the combustion process.

With temperature rising, between 200 ˚C and 400 ˚C, fuel suffers a thermal degradation – devolatilisation. Volatile organic matter is released from the biomass, mainly CO, CO_2 and H_2O, as well as pyrolytic products, mainly tar, leading to a slow loss of weight of the fuel material.

The remaining solid material of the fuel – charcoal – and the released volatiles are oxidised, while the temperature rises above 400 ˚C. Ideal combustion results in the maximum heat release from the fuel, minimizing losses from inefficient combustion, normally due to incomplete combustion and to deficient supply of air (oxygen). Hence, a good combustion process is accomplished by controlling the "three T's" of combustion which are (1) Temperature high enough to ignite and maintain ignition of the fuel, (2) Turbulence or intimate mixing of the fuel and oxygen, and (3) Time, sufficient for complete combustion.

An overall ideal reaction of biomass combustion can be defined by **Reaction (**1**)**:

$$\boldsymbol{C_nH_mN_oO_pS_qCl_r(H_2O)_s + g(O_2 + \varphi N_2)e_{air} \rightarrow aCO_2 + bH_2O + cNO_2 + dSO_2 + eO_2 + fN_2} \qquad \text{Reaction (1)}$$

Left side of the equation represents biomass and air, respectively. As a result of the combustion reaction, besides the combustion products (CO_2, H_2O, NO_2, SO_2, HCl and excess air O_2 and N_2), different types of pollutants are emitted:

1. Unburnt compounds such as CO, C_XH_Y, PAH, tar, unburnt carbon and PCDD/F;
2. Gaseous pollutants such as NO_X (NO and NO_2), N_2O, CO_2, SO_2 and HCl;
3. Ash particles containing Si, Al, Fe, Ca, Mg, Na, K, S, and P as well as heavy metals such as Zn and Pb.

The air mass needed for combustion depends on the chemical and physical characteristics of the fuel. In order to achieve a complete oxidation of the fuel the total flow of air (air_{total}) must be bigger than the stoichiometric flow (air_{stoiq}) demands leading to an excess air ratio, expressed in **Equation (1).** This excess of air must be controlled to avoid the process to cool down.

$$\%\boldsymbol{e_{air}} = \frac{\boldsymbol{air_{total}}}{\boldsymbol{air_{stoi}}} \times \mathbf{100} = \frac{\%\boldsymbol{O_2}}{\mathbf{21} - \%\boldsymbol{O_2}} \times \mathbf{100} \qquad \text{Equation (1)}$$

The pollutant emissions from biomass combustion are briefly explained in **Section 1.3**

1.2 COMBUSTION TECHNOLOGIES

Heat and electricity production technologies, using biomass as fuel, are well developed in many applications. Biomass heating systems range from domestic small-scale stoves (5 kW_{th} to 100 kW_{th}) to larger scale boilers for heat and power (100 kW_{th} to 500 kW_{th}). Large heat and power plants have capacities in the range of 1 MW up to 500 MW and are capable of using various biomass feedstock, *e.g.* wood residues, wood chips, straw, etc.

Thermal PPs use water as working fluid, in the form of steam. Steam generators, or boilers, use the heat to convert water into steam for power generation, by means of a steam turbine, and industrial process heating. Steam is a key resource because of its wide availability, advantageous properties and nontoxic nature.

The technological configuration of this type of PPs is based in Rankine's Ideal Cycle, which can be split into four subsystems (Babcock, 2005): Subsystem A is where the conversion from heat to work happens, the thermal energy in the working fluid is converted into mechanical energy in the turbine; Subsystem B is where the chemical energy from the fuel is converted into thermal energy, then stored in the working fluid; Subsystem C is where the energy stored in the working fluid is supplied to the cooling cycle; finally the Subsystem D, where the mechanical energy of the turbine is converted into electrical energy by the electrical generator.

The main feature of the Rankine cycle is that compression is confined to the liquid phase, avoiding the high compression work and mechanical problems. The temperature increase of the heat supplied to the working fluid in the boiler and the cooling temperature decrease in the condenser improve the thermal efficiency of the cycle. Hence, the working fluid, in steam state, is usually superheated in super-heaters systems.

The boiler is the component used in Subsystem B of a PP. The working fluid is mainly liquid water which gets into the vapour state, or steam. This high-pressured steam will then apply work in the steam turbine. The most common technology used to circulate the working fluid is the Aqua Tubular Boiler type, due to the high pressurized steam demands in a Power Plant. The fluid circulates inside the boiler by a pipe system and is heated from the outside by the combustion gases. The reverse is called Pyro Tubular Boiler.

Systems for biomass combustion can be distinguished by the flow conditions in the furnace: fixed bed combustion, bubbling fluidized bed (BFB) and circulating fluidized bed (CFB), and dust combustion (Nussbaumer, 2003), as shown in Figure 1.

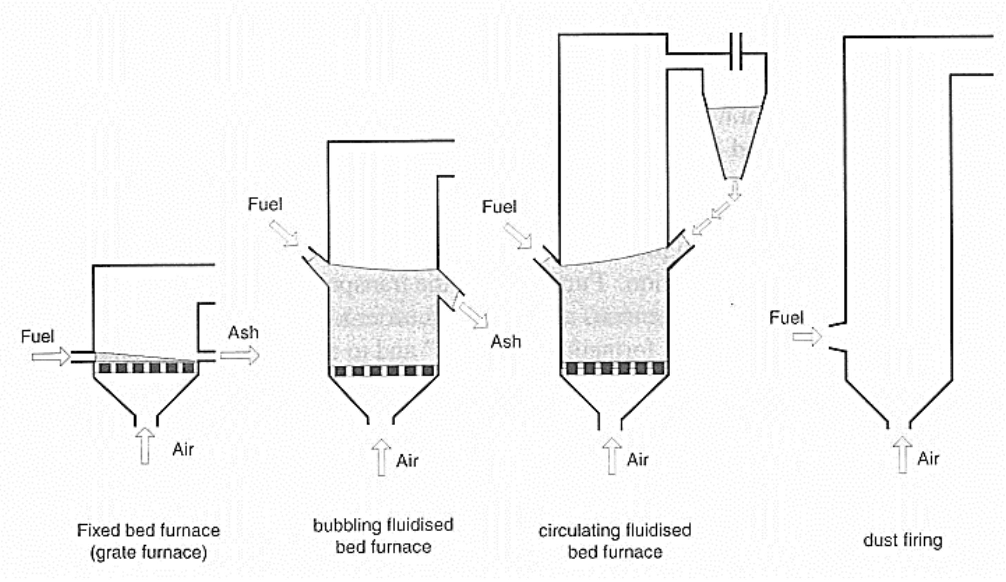

Figure 1 – Main combustion technologies for biomass (adapted from Van Loo et al. (2010))

These technologies normally have air staging systems, meaning that air supply is split, usually, into two inlets: primary and secondary, the first below and the last above the bed zone. This air staging enables good mixing of combustion air with the gases formed by devolatilization and gasification of fuel in the fuel bed zone. This mechanism allows controlling the combustion conditions and, therefore, controlling the pollutant formation and emissions. In conventional two-staged combustion, primary air is usually under stoichiometric, and a relevant residency time is needed between the fuel bed zone and the secondary air inlet (Nussbaumer, 2003).

Fixed bed combustion systems (T = 900 °C to 1200 °C) include grate furnaces and underfeed stokers. Primary air passes through a fixed bed, in which drying, gasification, and charcoal combustion takes place. The combustible gases produced are burned after secondary air addition has taken place, usually in a combustion zone above the fuel bed.

There are various grate furnace technologies available: fixed grates, moving grates, travelling grates, rotating grates and vibrating grates.

Grate furnaces are appropriate for biomass fuels with high moisture content, varying particle sizes, and high ash content. A good and well controlled grate is designed to guarantee a homogeneous distribution of the fuel over the whole grate surface. Furthermore, the transport of the fuel over the grate has to be as smooth and homogeneous as possible in order to keep the bed of embers calm and homogenous, to avoid the formation of “holes” and to avoid the elutriation of fly ash and unburned particles as much as possible (Van Loo *et al.*, 2010).

Dust combustion is suitable for fuels available as small particles (average diameter smaller 2 mm). A mixture of fuel and primary combustion air is injected into the combustion chamber, combustion takes place while the fuel is in suspension, and gas burnout is achieved after secondary air addition (Van Loo *et al.*, 2010).

1.2.1 FLUIDIZED BED BOILER

This technology is recognized as the most suitable for biomass combustion due to its low process temperatures, isothermal operating conditions, and fuel flexibility.

Within a FB, biomass fuel is burned in a self-mixing suspension of gas and solid-bed material into which combustion bed and circulating fluidised bed combustion can be distinguished. This type of boilers is applied in large-scale applications and often used for waste wood and industrial wastes, *e.g.* from the pulp and paper industry

A FB boiler consists of a compact vessel with an air distribution plate in the bottom, filled with a fluidized suspension bed of hot, inert, and granular material. The common bed materials are silica, dolomite and/or ashes from the fuel. The bed material usually represents 90 % to 98 % of the mixture of fuel and bed material.

Primary combustion air enters the furnace from below through the air distribution plate and fluidises the bed material so that it becomes a seething mass of particles and bubbles. Secondary air is introduced above the bed – splashing zone – and, usually, also further higher up – freeboard, also called tertiary air – by well distributed air inlets.

The combustion temperature has to be kept low (usually within 800 ˚C to 900 ˚C) in order to prevent ash sintering in the bed. This can be achieved by internal heat exchanger surfaces, by flue gas recirculation, or by water injection (Babcock, 2005).

As mentioned before, the primary air inlet induces an upward flow of a gas through a stacked height of solid particles, which will affect the pressure differential between the top and the bottom of the container, this is the fluidizing process. At high enough gas velocities, the gas/solids mass exhibits liquid-like properties, thus the term fluidized bed. The point where the bed starts to behave as a fluid is called the minimum fluidization velocity.

Regarding the minimum fluidization velocity, there can be four bed working regimes: Fixed bed - a small quantity of air flows through the air distributor into the sand; BFB - as the air flow increases further, bubbles of air start to form, and the bed becomes violent, increasing the bed volume. There is an obvious bed level and a distinct transition between the bed and the space above; Turbulent Fluidized Bed, by increasing the air flow further, the bubbles become larger and begin to coalesce, forming large voids in the bed. The solids are present as interconnected groups of high solids concentrations; CFB - a further increase in air flow causes the particles to blow out of the bed and the container. If the solids are caught, separated from the air, and returned to the bed, they will circulate around a loop. Unlike the bubbling bed, the CFB has no distinct transition between the dense bed in the bottom of the container and the dilute zone above. The solids concentration gradually decreases between these two zones (Babcock, 2005).

Regarding technological applications, fluidized bed boilers can be split into: CFB and BFB boilers, schemes of both are presented in **Figure 2**.

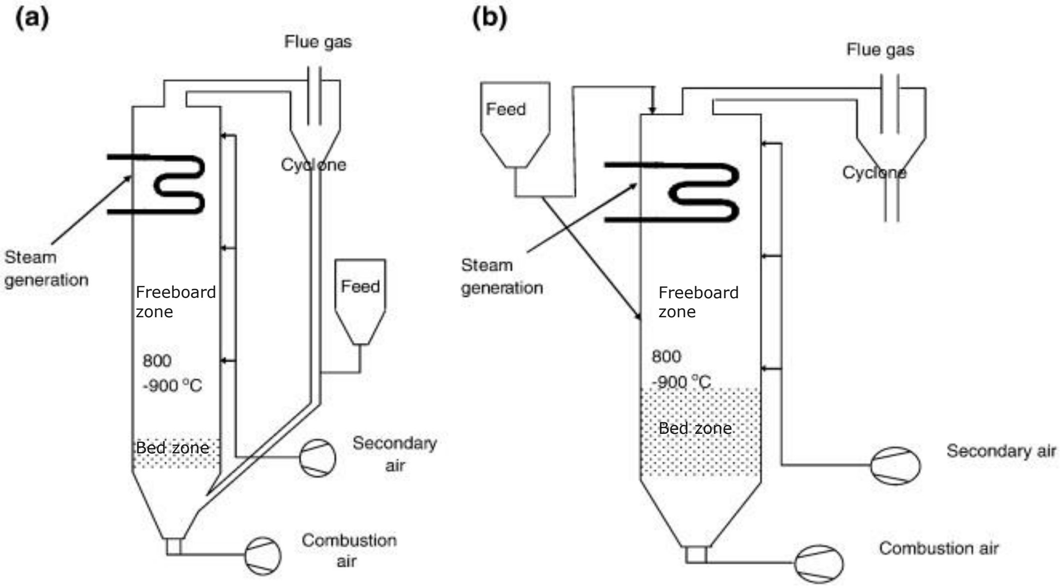

Figure 2 – *(a) Circulating Fluidized Bed, (b) Bubbling Fluidized Bed (adapted from Van Loo et al. (2010))*

The main differences between both are the fluidization velocity, bed particles' size, heat and mass transfer rate and flue gas composition profile along the reactor.

A CFB system is achieved with a fluidising velocity of primary air from 5 m/s to 10 m/s and using small sand particles, from around 0,2 mm to 0,4 mm in diameter, which are carried out of the bed zone. The sand particles will be carried with the flue gas, separated in a hot cyclone or a U-beam separator, and fed back into the combustion chamber. The high turbulence in CFBB leads to a better heat transfer and a very homogeneous temperature distribution in the bed, resulting in stable combustion conditions. In view of their high specific heat transfer capacity, this system are widely used at industrial scale, due to their higher combustion efficiency and the lower flue gas flow produced.

In a BFB the bed material is usually silica sand of about 1,0 mm in diameter; the fluidisation velocity of the air varies between 1,0 m/s and 3 m/s. In contrast to coal-fired BFB furnaces, the biomass fuel should not be fed onto, but into the bed by inclined chutes from the fuel hoppers because of the higher reactivity of biomass in comparison to coal. The advantage of BFB furnaces is their flexibility concerning particle size and moisture content of the biomass fuels. Furthermore, it is also possible to use mixtures of different kinds of biomass or to co-fire them with other fuels. One big disadvantage of BFB furnaces, the difficulty to work at partial load, is solved in modern furnaces by splitting or staging the bed (Van Loo *et al.*, 2010).

Due to the good mixing achieved, FB plants can deal flexibly with various fuel co-firing, but are limited when it comes to fuel particle size and impurities contained in the fuel. Therefore, appropriate fuel pre-treatment system covering particle size reduction and separation of contaminants (metals, stones and soil) is necessary for fail-safe operation. Moreover, partial load operation of FB combustion plants is limited due to the need of the bed fluidisation.

The intense heat transfer and mixing provides good conditions for a complete combustion with low excess air demand: between 1,1 and 1,2 for CFB plants and between 1,3 and 1,4 for BFB plants (Babcock, 2005).

One disadvantage of FB combustion plants is posed by the high dust loads entrained with the flue gas and the fuel, mainly biomass, which make efficient dust precipitators and boiler cleaning systems necessary. Bed material is also lost with the continuous ash extraction, making it necessary to periodically add new material to the plant.

1.3 EMISSIONS FROM BIOMASS COMBUSTION

This section presents a brief description regarding some of the pollutant emissions and mechanisms – CO, NO_x, SO_2, HCl and Particulate Matter (PM) in particular – are presented.

According to the European Directive (2010/75/EU) on industrial emissions (IED), the term "pollution" means the direct or indirect introduction, as a result of human activity, of substances, vibrations, heat or noise into air, water or land, which may be harmful to human health or the quality of the environment, result in damage to material property, or impair or interfere with amenities and other legitimate uses of the environment (IED, 2010).

The pollutant emissions considered by the IED, for biomass combustion, are PM, NO_x and SO_2. Nevertheless, CO and HCl emissions were taken into consideration.

1.3.1 LEGAL FRAMEWORK

The European Union addresses air pollution through a number of legal measures. The Large Combustion Plant Directive (LCP) (2001/80/EC), transposed to Portuguese law by Decree-Law 178/2003, de 5 de Agosto, sets the main principles for the permitting and control of installations with rated thermal input of 50 MW_{th} to 100 MW_{th}.

This directive is based on an integrated approach and the application of Best Available Techniques (BAT, 2006). These are the most effective techniques to achieve a high level of environmental protection, taking into account the cost and benefit. For combustion systems BAT for LCP was published in the 2001 Reference Document on Best Available Techniques for Large Combustion Plants (BREF, 2006). On 7 January 2014 the IED, transposed to Portuguese law by the Decree-Law 127/2013, of August 30, repealed and replaced Directive 2008/1/EC on Integrated Pollution Prevention and Control (IPPC), Directive 2000/76/EC on Waste Incineration (WID), Directive 1999/13/EC on activities using organic solvents and Directives 78/176/EEC, 82/883/EEC and 92/112/EEC, concerning titanium dioxide production.

Furthermore, in order to complete the regulatory framework for the combustion sector, in December 2013 the Commission adopted a proposal for a new Directive to control emissions of air polluting substances from combustion plants with a rated thermal input between 1 MW_{th} and 50 MW_{th}.

Therefore, a Medium Combustion Plants (MCP) directive proposal was presented. With this, the Commission aims to avoid possible trade-offs between air quality and increased biomass use, which may otherwise result in increased air pollution (MCP, 2013).

In the proposed Directive (MCP, 2013), on the limitation of emissions of certain pollutants into the air from MCP, it is stated that from 1 January 2025 emissions into air of SO_2, NO_x and PM, from an existing medium solid biomass combustion plant with a rated thermal input above 5 MW_{th}, must be controlled.

Also another proposal is in works, this one to transpose into EU law the international emission reductions for 2020, that the EU has committed to under the 2012 Gothenburg Protocol of the Convention on Long-Range Transboundary Air Pollution (LRTAP, 2014). The LRTAP protocol aims to control emissions of heavy metals, by establishing ELVs, caused by anthropogenic activities that are subject to long-range transboundary atmospheric transport and are likely to have significant adverse effects on human health or the environment. However, this protocol only applies to large combustion plants (>50 MW_{th}) and shall not apply to plants using biomass as their only fuel source.

In the scope of the Air Quality, the objectives related to limit value and exposure – exposure concentration obligation and exposure reduction target − for gaseous pollutants (SO_2, NO_x, CO) and $PM_{10/2,5}$ are specified in Directive 2008/50/EC on ambient air quality and Cleaner Air For Europe (CAFE), transposed to the Portuguese law by Decree-Law 102/2010, on September 23. The information on all air pollution abatement measures that have been considered at appropriate local, regional or national level for implementation in connection with the attainment of air quality objectives, include, among other, reduction of emissions from stationary sources by ensuring that polluting small and medium sized stationary combustion sources (including for biomass) are fitted with emission control equipment or replaced (AAQ, 2008).

Within the Portuguese framework the prevention and control of SO_2, NO_x, CO and TSP emissions was established by the Decree-Law 78/2004, of April 3. It comprises combustion plants whose rated thermal input is greater than 100 kW.

In Portugal Emission Limit Values (ELV, mg/Nm^3) are fixed by Portaria 675/2009, of June 23rd (general ELV) and Portaria 677/2009, of June 23 rd (fuel specific ELV). In addition, pollutants maximum mass flow limits, fixed by Portaria 80/2006 of January 23 rd, are 50 kg/h for SO_2, 30 kg/h for NO_x and 5 kg/h for PM.

The ELVs for biomass combustion, from the European IED and the new MCP directive proposal and the Portuguese Decree-Law (DL) 78/2004, of April 3 rd, are presented in **Table 3**.

Table 3 *– Emission Limit Values (mg/Nm^3) for biomass combustion, in Europe and Portugal*

	Europe			Portugal	
	IED		MCP	DL 78/2004	
(mg/Nm^3)	6 % O_2	11 % O_2	6 % O_2	8 % O_2 [2]	11 % O_2 [3]
PM (dust)	30	-	30	150	-
SO_2	200	-	200	500	-
NO_x	300	-	650	-	650
CO	-	100[1]	-	-	500

[1] Hourly average value for waste incineration plants using fluidized bed technology
[2] Portaria 675/2009, 23rd June
[3] Portaria 677/2009, 23rd June

In IED the ELV for HCl is 10 mg/Nm^3 at 10% O_2 for waste incineration and co-incineration. In the previously mentioned regulation, applicable to combustion systems, HCl is not regulated, however this ELV will be considered, as a reference value. The Portuguese DL 78/2004, defines a general ELV for chlorine compounds emissions of 30 mg/Nm^3 at 8% O_2 (around 25,4 mg/Nm^3 at 10%O_2).

1.3.2 CO EMISSIONS

Carbon monoxide (CO) emissions are essentially the result of incomplete combustion, hence belonging to the unburnt pollutants. Its emissions are usually related to the combustion efficiency, because of its dependence on the operational parameters related with the mentioned “three T’s” of combustion – Temperature (around 850 °C), Turbulence and Time of residence (around 0,5 s) – and fuel feeding characteristics such as compositions and granulometry. Therefore, it is possible to control its emissions by controlling these parameters.

In FB boilers, CO emissions are reduced by using air staging, running the system at lower fluidization velocity (increased residence time) and lower sand particle size as bed (providing good mixing at low fluidization velocities) (Khan *et al.*, 2008). In terms of CO emissions, FB possess formation and destruction zones of CO. The formation zone in the boiler bed, were the early combustion stages take place, while the destruction zone is usually in the freeboard where the second air oxidizes the CO with OH and HO_2 radicals and also O_2 directly.

Small scale biomass units can produce higher emission concentrations because of the fuel's high volatile content and the unit's shorter freeboard: leading to an insufficient residence time inside the furnace to combust, regarding the amount of produced volatiles. Hence, the importance of air staging, which can reduce unburnt pollutants to levels close to zero (Nussbaumer, 2003). The heat exchangers, that might be located inside the freeboard, decrease the temperature of the gases, inhibiting the conversion of CO to CO_2. Also, irregular or improper fuel feeding could lead to higher CO emissions (Gulyurtlu, 2004).

1.3.3 NO_X EMISSIONS

Nitrogen base pollutants are commonly summarized as nitrogen oxides (NO_x) and refer to the nitrogen oxide (NO) and nitrogen dioxide (NO_2) formed during the combustion process. NO is the main form produced and emitted, around 30 %, and is converted to NO_2 in the atmosphere (Obernberger *et al.*, 2006). This pollutant generates a high environmental concern as an air pollutant due to its influence in acid rain, eutrophication and haze. Its formation process can be summarized into three steps:

1. Thermal NO: formed from the nitrogen of air, in high temperature conditions (typically >1300 °C) due to dissociation of the atmospheric diatomic specie N_2;
2. Fuel NO: formation as a result of reactions involving fuel bound N;
3. Prompt NO: formed by fast reactions between the nitrogen of air, N_2, and fuel bound hydrocarbons radicals. This reaction forms intermediate reactants, *e.g.* HCN, which are later oxidized into NO.

For biomass combustion, fuel-bound nitrogen is the main source of NO_x emissions. Thermal and prompt NO_x represent a small share due to the typical lower temperatures of biomass combustion in FB (below around 900 °C) (Nussbaumer, 2003).

Due to the low combustion temperatures, when compared with other combustion systems, formation of N_2O may also occur in FB systems. N_2O, although in much less quantities, contributes to the greenhouse effect and ozone depletion. The intermediate volatiles formed during biomass combustion in FB, mostly NH_3 and HCN, are the dominant source of NO_x and N_2O, that react with oxygen while still in the bed. On the other hand, if no oxygen is available, intermediates can interact in the freeboard forming N_2. Also, the presence of CaO, MgO, and Fe_2O_3 in the fuel can lead to the formation of an active bed that can catalyse the reduction of NO and N_2O, especially under fuel-rich combustion conditions (Khan *et al.*, 2009).

There are two ways of reducing NO_x: primary measures, also known as *in-situ* reductions, are based on the combustion process control, minimizing the NO_x formation. The main technics used in biomass combustion are low working temperatures, air staging and, fuel staging leading to oxygen and temperature control, with NO_x reductions between 30 % to 80 % (Nussbaumer, 2003). Flue/Exhaust Gas Recirculation is also an option, although with minor influence on NO_x emissions.

Reburning is also a widely used solution. This technology consists in using auxiliary burners with a secondary fuel, usually natural gas, in the zone above the primary combustion zone (bed). Reduction of NO_x occurs in reaction with the hydrocarbon fragments (CH and CH_2) formed in the secondary fuel combustion.

Secondary measures can be used, if the emission limits are not met with the primary emission reduction measures. These are: Selective Catalytic Reduction (SCR) that consists in ammonia (NH_3)or urea injection over a catalyst at about 250 °C to 450 °C, with reduction efficiency up to 95 %; Non-Selective Catalytic Reduction where the ammonia injection takes place in a separate reduction chamber at 850 °C to 950 °C, reduction efficiencies up to 90 % (Khan *et al.*, 2009).

1.3.4 CHLORINE EMISSIONS

During combustion mainly gaseous HCl, and also Cl_2 and alkali chlorides such as KCl and NaCl are produced. Due to subsequent cooling, part of Cl condenses as salts on fly ash particles in flue gas or in heat exchangers surfaces. The incorporation of Cl in the ash, which may attain 40 % to 80 % for wood combustion, depends on availability of alkali, earth-alkali metals present in the fuel (Obernberger *et al.*, 2006). Chlorine (Cl) emission are not considered by the IED, although their emissions might relevant in case of a high Cl content fuel.

HCl retention may be achieved with CaO or $CaCO_3$, when limestone or dolomite are used as sorbent in FB. The end product of limestone chlorination is found to be $CaCl_2$ between 650 ^{o}C and 850 ^{o}C, with a molar Ca/Cl ratio above 2 (Partanen *et al.*, 2005a).

Beside emissions, other important effects of Cl are corrosion of metal parts in the boiler (expected for concentration above 0,1 wt% d.b.) (Obernberger *et al.*, 2006), promoting emission of heavy metals as fine particles, because Cl promotes the volatility of heavy metals (Zn, Ni, Cu, Fe, Cr, Pb chlorides) (Lopes *et al.*, 2009). Cl may also lead to emission of dioxins and furans (PCCD/F).

1.3.5 SO_X EMISSIONS

Fuel bound sulphur generates gaseous compounds, mainly, sulphur dioxide (SO_2) and minor quantities of sulphur trioxide (SO_3). It can also be retained in solid forms as metal sulphates during the combustion process (Obernberger, 2005). This pollutant is known as one of the causes of acid rain. Together with chlorine, it may cause corrosion of boiler components, which is a major concern when compared with its low emissions, in biomass combustion systems.

During devolatilization of the fuel, sulphur can be released as H_2S, in reductive zones, being later oxidized by the combustion air (Tarelho *et al.*, 2005). The sulphates may condensate on the fly ash particles' surface in a rapid cooling of flue gas flow.

Co-combustion experiments of biomass and coal led to conclude that SO_X emissions reduce with the increase of biomass share, due to the lower sulphur content of biomass. Biomass increases the SO_2 retention as a result of its ash high content of alkaline compounds K_2O, Na_2O, CaO and MgO (Fuertes *et al.*, 1992). Studies have shown that from 40 % to 90 % of the sulphur is retained by the fuel's ash (Obernberger *et al.*, 1997). In FB systems, due to the low operating temperatures, sulphur tends to remain as $CaSO_4$ form, minimizing SO_2 emissions, therefore the presence of S may interfere with the alkali metals' behaviour.

In FB, SO_x emissions can also be controlled by *in-situ* addition of limestone, with $CaSO_4$ as the main product, at temperatures in the range of 800 °C to 900 °C. Also, dolomite is a common used sorbent, producing Ca sulphate. SO_2 reductions of 90 % to 95 % are typically achieved in CFB, which is normally enough to achieve the emission limits.

Retention efficiency of SO_x in the FB is highly dependent on operating conditions: limestone's particle size, system's temperature and residency time. A high retention is achieved by small particles of the sorbent, providing a larger surface area, and decreases for bigger particles at the same temperature ranges. Low temperatures, between 675 °C and 725 °C, showed the best sulphur retention regardless the particle size, and is the indicated range of temperatures for absorption by larger particles (Laursen *et al.*, 2002). This study concluded that 3:1 Ca/S is an ideal molar ratio for sulphur retention by limestone.

Simultaneous retention of HCl and SO_2 with limestone was studied, concluding that both compete for unreacted Ca leading to limestone chlorination suppression while its sulphation is enhanced (Partanen *et al.*, 2005b), *i.e.* the presence of HCl promotes the SO_2 capture by the bed material.

1.3.6 PARTICULATE MATTER EMISSIONS, $PM_{10/2,5}$

The control of Particulate Matter (PM) emissions is one important concern in biomass combustion systems. The United States Environmental Protection Agency (EPA, 2013) states that PM *includes both solid particles and liquid droplets found in air. Many anthropogenic and natural sources emit PM directly or emit other pollutants that react in the atmosphere to form PM. These solid and liquid particles come in a wide range of sizes.*

PM, referring to particles emitted with the flue gases of power generation plants, depend on the fuel characteristics, such as: composition; particle dimension and morphology; combustion technology system characteristics. These particles are generally classified into two classes: particles from incomplete combustion, such as soot, tar and char, and particles from inorganic material in the fuel's ash, commonly referred as fly ash (Khan *et al.*, 2009).

The first class can be easily managed by improving the combustion conditions, since its formation occurs early in the flame zone. Particles formed by inorganic material are divided into coarse fly ash and aerosols, corresponding to larger particles and smaller particles respectively.

During combustion the biomass particle undergoes various mechanisms resulting in the mentioned particles, as shown in **Figure 3**. The ash constituents' elements have different behaviours during combustion process, according to their volatility.

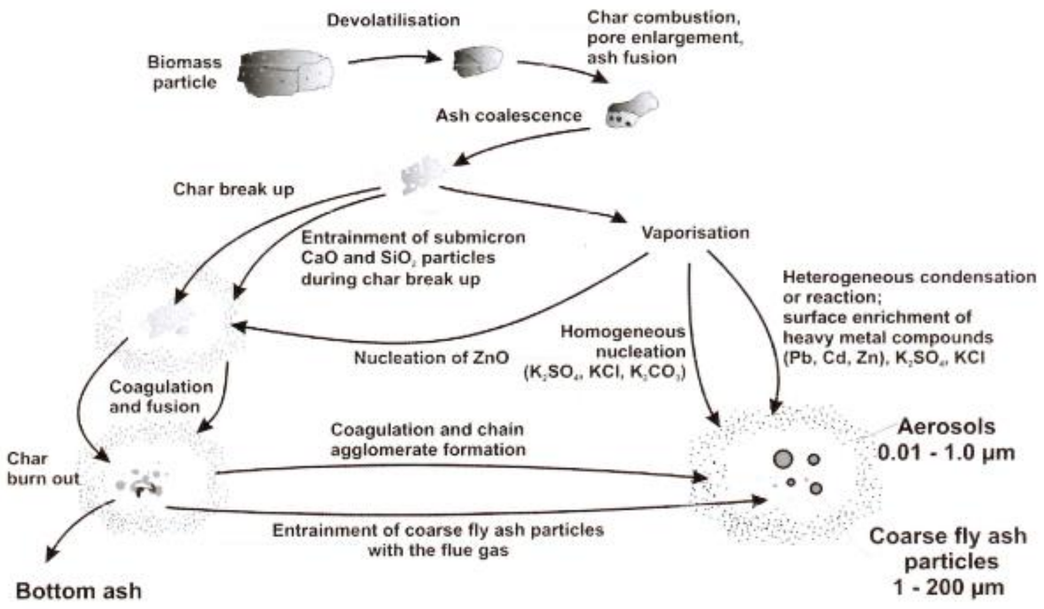

Figure 3 - *Ash formation during biomass combustion (adapted from Obernberger (2005))*

Coarse fly ashes are mostly produced from transport of minerals contained in biomass and also fusion and coagulation mechanisms of non-volatile ash elements such as Si, Ca, Mg, Al, P and Fe. This mechanism consists in the agglomeration of both regular and irregular shape particles through the outer layer (Khan *et al.*, 2009). It is common that alkaline and heavy metal salts, form aerosol particles, and condensate on the surface of the coarse particles.

Aerosols are mainly originated by easily volatile elements, normally heavy metals and alkali metals, under nucleation and condensation mechanisms (Nussbaumer, 2001). A great share of these constituents is released into the gas phase, at high temperatures, going through homogeneous gas phase reactions and ultimately nucleate, due to super saturation (Obernberger, 2005).

Aerosol particles can form coarser particles through heterogeneous condensation on other particles' surfaces; coagulation of particles and growth; explosions of cenosphere (round, hollow vitrine-derived particles); aerodynamic transport of small mineral forms and unburned matter (Lopes *et al.*, 2009).

In the case of biomass combustion in FB, ultra-fine particles are mainly formed by alkali sulphates and chlorides nucleation and condensation on particles with metal oxides. Alkali compounds have low melting temperatures, that when condense may form low viscosity sticky layer, that highly contributes to the deposition of impacted particles (Nussbaumer, 2001).

Due to high volatility of Cd, Zn, and Pb, even small amounts of these heavy metals can appear in the aerosols, especially from waste treated wood.

A correlation between CO and PM emissions can be related to the fuel incomplete combustion, leading to soot formation, emitted as PM with the flue gas (Henriques, 2013). The same author found that the increment of air staging influences the $PM_{2,5}$ emission, by reducing it.

During efficient combustion of solid biomass, *i.e.* under stable conditions, resulting in low CO emissions, ultrafine particles (<100 nm) production is uniform, generating unimodal particles distribution. On the other hand, combustion with medium and high CO emissions present bimodal particles distribution and higher diameters (>100 nm): the higher the CO emission is, the higher the particles diameter is (Torvela *et al.*, 2014).

Particles are classified on aerodynamic particle size class basis: Supermicron particles present diameters typically between 1 µm and 100 µm; Submicron particles in the diameter range below 1 µm. The particle size distribution in FB burning biomass is generally bimodal, with one submicron and one supermicron maximum, as shown in **Figure 4.**

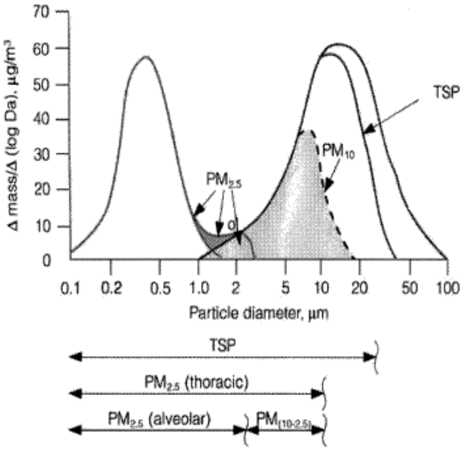

Figure 4 - Particles concentration distribution by diameter (adapted from Sloss et al. (2000))

TSP stands for Total Suspended Particles and, as well as $PM_{10/2,5}$, has standardized sampling methods, which will be described in **Section 2.3.**

The total range (0,1 µm to 100 µm), shown in **Figure 5** – $PM10_{/2,5}$ particles size comparisons with sand and hair**,** may be classified as: Inhalable particles, for particle that get retained in the respiratory system; Thoracic particles, with medium aerodynamic diameter of 10 µm or smaller (PM_{10}) ,that can be retained the lungs and Alveolar particles, are the smaller range of particles of 2,5 µm and below ($PM_{2,5}$), can get retained in the alveoli; and might also be transported into the blood stream.

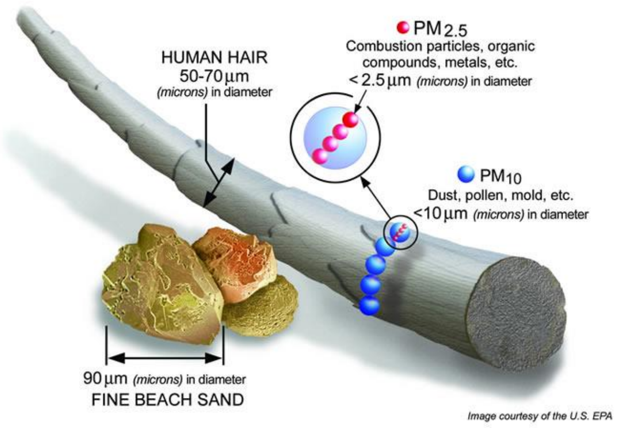

Figure 5 – *$PM_{10/2,5}$ particles size comparisons with sand and hair*

The high amounts of K, Na and Cl, that may be present in some biomass, lead to a large emission of submicron particles, when compared with coal combustion in FB systems. This might be attributed to the production of higher quantities of aerosols of KCl and NaCl, with diameters below 1 µm (Lopes *et al.*, 2009).

Another used nomination for submicron ultrafine particles with diameter of 1 µm and lower is PM_1 (Torvela *et al.*, 2014).

Health problems might come from this range of particle sizes, since they may remain suspended in the atmosphere for days or weeks. Exposure to fine particles can be toxic and has been associated to cases of premature mortality. Other reported effects include aggravation of respiratory and cardiovascular disease, lung disease and decreased function, asthma attacks and certain cardiovascular problems (EPA, 2013).

Besides the particle diameter, the deposition fraction in the respiratory-tract also varies depending on the hygroscop and solubility of the particle. Approximately 20 % of particles emitted from biomass combustion are deposited in the respiratory-tract, a relatively low percentage when compared to the expected deposition of fresh traffic exhaust particles. This occurs due to the hygroscopic material in the biomass particles, salts and water-soluble organic species, in contrast to the hydrophobic traffic exhaust particles (Londahl *et al.*, 2008).

1.4 PARTICLE CLEANING TECHNOLOGIES

Concerning biomass combustion, the post-combustion flue gas treatment is mainly focused on the particles emissions. Particle removal from flue gas can be divided in two main methods: dry methods and wet methods (Singh *et al.*, 2014). Dry methods include cyclones, dry electrostatic precipitator (D-ESP), fabric filters or baghouse and electrified gravel (sand) bed filter. The main wet systems for particulate removal are wet electrostatic precipitators (W-ESP), electrified wet scrubber (EWS), scrubbers and mop fan.

In dry removal methods for flue gas cleaning no liquid is used, method is either based on inertia principle, *e.g.* cyclones, electrical properties of particles in electrostatic precipitators, filters based on permeability principles, and others.

In wet methods of flue gas cleaning, liquid is used as an agent to extract the contaminants or pollutants from flue gas. Also many gaseous contaminants are water/liquid agent soluble and use that property for removal. Major disadvantage of such types of system lies in the recycling of the collected contaminated liquid used for cleaning of the flue gas. This provides another major challenge to reduce the quantity of liquid used for cleaning purpose.

1.4.1 CYCLONES

Mechanical/inertial collector characteristics limit its use to small or medium sized installations. Cyclones are mainly solid–gas separation systems widely used in different industries, very useful as pre-cleaning devices of particles larger than 10 µm aerodynamic diameter (Lee *et al.*, 2008).

A cyclone is a cylindrical vessel, usually with a conical bottom. The flue gas is fed into the vessel tangentially and gains a rotary motion whirling in a circular or conical path. The particles are thrown against the walls by the centrifugal force of the flue gas motion, generating a vortex, where they impinge and eventually settle into hoppers. It is possible for high efficiency cyclones to achieve collection efficiency up to 70 % for particles of 5 µm size, however the collection efficiency decreases rapidly when size of pollutant particles reduces further (Naylor, 2009), although, at high temperature and pressure cyclone’s performance is more efficient even for fine particle size of 2 µm to 3 µm. Cyclones are robust and can deal with cyclic operation and load changes, which is quite common in these types of plants. Their global efficiency is moderate when compared with D-ESP or fabric filters.

Theoretical development and experimental validation of optimized recirculating reverse flow gas cyclones conclude that, by partially recirculating the cyclones' emissions, a high collection of submicron particles is observed even for lower inlet concentrations (as low as 100 mg/m^3) (Salcedo *et al.*, 2007).

1.4.2 DRY ELECTROSTATIC PRECIPITATORS

D-ESP are typically used after a mechanical particle collector to reduce the particulate concentration in the flue gas. D-ESP are extensively used as suitable pollutant control systems. Their major merits of high collection efficiency and wide range of operating temperatures makes them the appropriate solution for various applications in industry (Castle, 2001).

The system comprises of a series of parallel, vertical metallic plates – Collecting Electrodes (CE) – forming ducts through which the flue gas passes. Centred between the CE – positive polarity – are the Discharge Electrodes (DE) – negative polarity. An electric field is established in the region between both Electrodes. The pollutant particles are given a negative electric charge by passing through that region, where gaseous ion flow – corona – is generated, due to the high voltage. The negatively charged particles are attracted toward the CE and separated from the gas flow, accumulating there. Generally, D-ESP has collection efficiencies of 99,5 % to 99,9 % for coarse particles, but for fine particles the collection is lower (Naylor, 2009). That fact is related to the particle size and its charging relation. Also, the gas velocity is an important factor in terms of the efficiency of these units. Hence, smaller particles that are of greatest environmental and health concern are collected with the lowest efficiency, which is the major limitation of D-ESPs. Possible high carbon content in fly-ash or CO, may require reducing the potential in the precipitator, or even interrupt. It is necessary to ensure no tramp air enters the precipitator and that the fly-ashes area continuously removed from the hoppers (Babcock, 2005). The operation temperature range is around 130 °C to 180 °C.

After being collected by the CE, the particles build up a layer of dust on the electrode surface which is dislodged by mechanically striking the collection surface. The dislodged particles fall by gravity towards the bottom of the precipitator, ending up in the bottom hopper from where the dust is extracted by either mechanical conveyor or pneumatic type system.

Many types of D-ESPs have improved functionalities, *e.g.* single stage, multi stage, D-ESP agglomerators, D-ESP with modified electrode and many others (Singh *et al.*, 2014).

1.4.3 FABRIC FILTERS OR BAGHOUSE FILTERS

Fabric filters (FF) have not been very widely used in removal of particulates from biomass combustion due to its fire potential (Babcock, 2005). One of the major advantages of this technology is that high removal efficiency of particulate is almost independent of size distribution of particulates in flue gas.

The FF is comprised of a multiple compartment enclosure with each compartment containing up to several thousand long, vertically supported, small diameter fabric bags. FF is a very successful option used where not only particulates but also gaseous impurities, *e.g.* SO_2, HCl, etc., need to be removed. However one major limitation of fabric filter is that flue gas must be dry otherwise particulate cannot be removed properly from gas and filter clogs. The bag cleanability and high pressure drop, which has resulted in conservatively designed, large, costly FF, may also be problems to consider.

Many modified filters are reported in the literature, *e.g.* electrified sand bed filter (Duarte Fo *et al.*, 2000), electro filters (Nifuku *et al.*, 2001), electrically energized fibrous filter, electrically energized granular-bed filters (Jaworek *et al.*, 2007) etc. These electrically charged filters claim to achieve removal efficiency of up to 99,97 %.

1.4.4 SCRUBBERS

Wet scrubbers have been a widely used technology for removal of particulate matter, and also acidic gasses and mist from flue gas, mainly due to its low capital cost, when compared to D-ESPs and FFs. Also, they do not require very complicated design and are easily maintained.

Wet scrubbers function is to inject water droplets into the flue gas to form a wet flue gas stream. The addition of limestone to the water can be done in case of high SO_2 emissions. The water used as a scrubbing agent is presented as a disadvantage because of the pollution and foul smell due to deposition of salt and associated cost in treating the sludge before disposal (Singh *et al.*, 2014). Also, there is the need for a wet ash collection system and a water separation and clarification system. Another drawback is the flue gas cool down during wet scrubbing, which may require gas reheating, and suffers a considerable pressure drop, resulting in fan power increase, meaning higher energy costs. Partly due to such operating costs, the use of wet scrubbers for the control of particulate emissions has decreased lately.

Other types of scrubbers for flue gas cleaning have been developed, *e.g.* venturi scrubbers, nozzle scrubbers, wet electrostatic scrubbers and wet scrubbers with condensation.

In electrostatic wet scrubber electric charging of water sprays is done by using electrostatic nozzles. It is reported that when particles and water spray are charged, comparing with non-charged, the cut size of scrubber is reduced from 2,5 µm to 0,25 µm (Schmidt *et al.*, 1992).

1.4.5 WET ELECTROSTATIC PRECIPITATOR

W-ESP are claimed to be one of the most effective separators of particulates, differing from the D-ESP in both materials and configuration; however the collection mechanism is basically the same. One major benefit, when comparing W-ESP and D-ESP, is that dust resistivity does not play major role.

The dust is absorbed in liquid and drained off from the collecting plates. This advantageous feature of W-ESP enables them to design for high level of dust removal efficiency. In many W-ESP membranes collection electrodes, consisting of silica or carbon fibres, are used (Bayless *et al.*, 2004). Typical operation is at or below the flue gas acid moisture dew point temperature for the gas being filtered. Collection efficiencies of 99 % have been reported with wet ESPs when precipitator sections or modules are placed in series (Babcock, 2005).

Hybrid Systems

The various techniques discussed in previous sections have some major advantages and disadvantages. The attempt to integrate the best principle of each technology led to the research of hybrid devices. Some of them are briefly described.

Compact Hybrid Particulate

In the Compact Hybrid Particulate Technology (COHPAC^{TM}) a high ratio pulse jet fabric filter collector is installed in series with an existing, energized D-ESP, serving as the polishing or final collection device. As the D-ESP removes the majority of ash prior to entering the fabric filter, the filtration rate can be increased substantially, while still maintaining the same pressure drops as conventional filtration systems (Chang, 1992).

Advanced Hybrid Particle Collector

Advanced Hybrid^{TM} Particle Collector (AHPC) combines electrostatic precipitation with fabric filtration, instead of placing the D-ESP and fabric filter sections in series, the filter bags are placed directly between the D-ESP collection plates. The collection plates are perforated (45% open area) to allow dust to reach the bags, however, because the particles become charged before they pass through the plates, over 90% of the particulate mass is collected on the plates before it ever reaches the bags (Miller, 2003).

Multi Stage Collector

The Multi Stage Collector (MSC™) combine the best features of the two-stage D-ESP and a Barrier Filter (BF) and provides a synergistic combination of both single- and two-stage electrostatic precipitation while incorporating an additional collector-stage by filtering the gas exiting the collector through a barrier collector-zone (Krigmont *et al.*, 2008). The MSC™ contains multiple narrow and wide zones formed by parallel corrugated plates. Enclosed in the narrow zones are discharge electrodes which, by corona discharge, charge the particulate matter. Particles removal efficiency increases at downstream zones, after repeated stages in series.

Electrocyclone

The use of electrical forces can increase the collection of fine particles, when an electrode can be placed in the axis of a cyclone – electrocyclone (Lind *et al.*, 2003). Collection efficiency reduces significantly when flow rate is too high.

Novel swirl cyclone

Novel swirl cyclone consists of cyclone, swirl plates, scrubber, feeding mechanism, scrubbing medium, demister and a circulation device. (Lee *et al.*, 2008). Gas stream first passes through the cyclone zone, it goes to swirl plate’s zone and then wet scrubber is utilised over them.

A synthesis of the main particulate removal technologies efficiency and particle size range is presented in Table 4.

Table 4 – Comparison of major particle cleaning technologies (adapted from Singh et al. (2014)).

Technology	Effectiveness (coarse particles) (%)	Removal efficiency (PM_{10}) (%)	Removal efficiency ($PM_{2,5}$) (%)	Achievable final PM emission (g/GJ)	Remarks
Cyclone	90-99	80-90	<80	30	Less effective for small particles
Multi-cyclone	90-99	90-99	<80	30	Less effective for small particles
ESP	>99	>99	80-90	15	Removal efficiency may be low for small plant
Fabric Filter	>99	>99	>99	<15	Final emission should be much less
Hybrids	>99	>99	>99	<15	Novel technology are more niche and problem specific

2 WORK DEVELOPMENT

The experimental work focused on the *in situ* sampling of particulate matter and other pollutants emissions from an industrial biomass-fired power plant. Flue gas was characterized, following standard sampling methods, which are later explained.

Previously to the field work, characterization of the PP and of the fuel were done, in order to understand and predict the combustion and emissions behaviour. Excess air and flue gases were theoretically determined and compared to the gases analysed by monitoring system, also relevant to understand the combustion process.

The sampled particulate matter were chemically and morphologically characterized by SEM analyses.

2.1 POWER PLANT CHARACTERIZATION

The experimental work was developed in a biomass-fired thermal power plant, located in a portuguese pulp and paper industry, in the scope of the BiomAshTech project. The power plant schematic representation is similar to the one shown in **Figure 6**.Thermal capacity of the BFB is between 20 MW_{th} and 50 MW_{th} with an average bed temperature in the range of 850 ˚C to 870 ˚C, and average expanded silica sand bed height in the range of 0,50 m to 0,75 m.

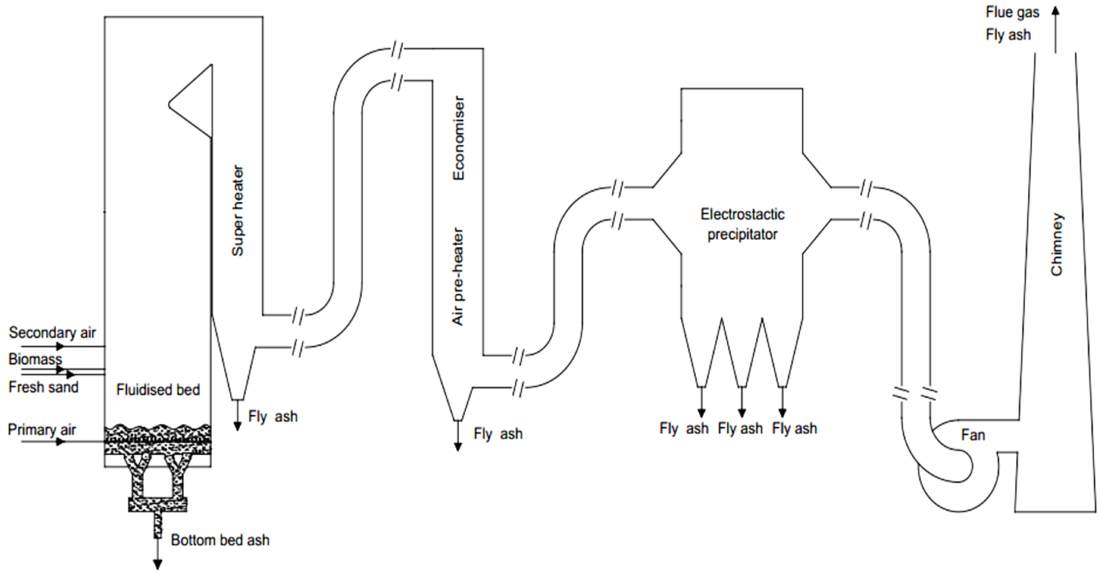

Figure 6 **–** *Industrial Unit scheme (adapted from Tarelho et al. (2013))*

The combustion air is staged at two levels: primary air injected below the sand bed and secondary air injected above the biomass feed point. Excess air in the FB, determined by **Equation (1)** for the periods of sampling, varied from 23 % to 46 %.

Flue gas cleaning is done by a three field D-ESP, assuring a particulate emission below 3 mg/Nm^3 (d.b., 8% O_2) in normal operating conditions (Data from PP).

The unit's chimney has a height of *ca.* 60 m and an internal diameter of 1,4 m and is equipped with a working platform surrounding its full perimeter at 20 m high. It has two access ports to the flue gas duct, located 90˚ of each other. A Continuous Emissions Monitoring Systems (CEMS) is installed in the stack at that same level.

2.2 BIOMASS CHARACTERIZATION

Biomass used in the studied unit accounts *ca.* 70 % of its origin from the Industrial Partner's internal activities, of wood debarking, while the remaining share is ensured from outside sources (Data from PP). **Figure 7** presents the morphology of biomass consumed at the PP during the sampling period.

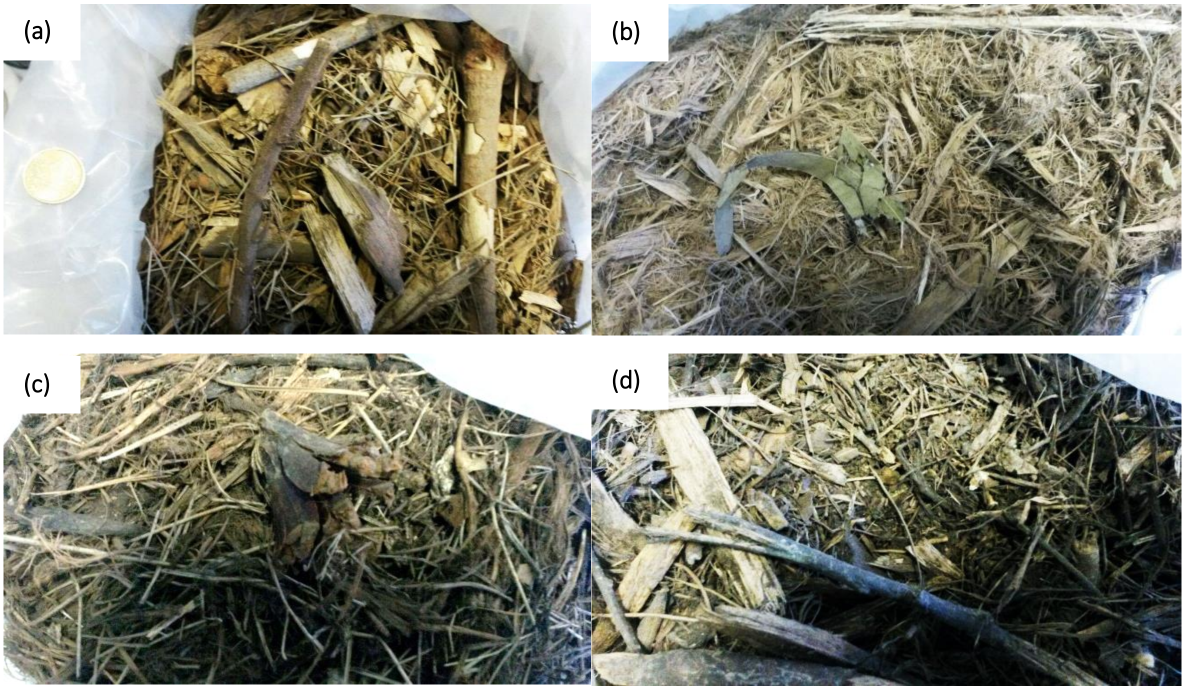

Figure 7 – Biomass samples from the Industrial Unit. (a) and (c) Pine; (b) Eucalyptus, (d) Mixtures

Biomass feedstock is a heterogeneous mixture of forest biomass residues from forestry related activities. Mainly species detected are eucalyptus **(b)** and pine species **(a, c)** with leaves, bark, conifer cone, needles and branches of various dimensions. Also a mixture of species **(d)** with pine needles and branches from other species. It was possible to observe the wide variation of fuel granulometry and presence of stones and soil particles.

The boiler capacity is *ca.* 18 tonne of fuel per hour (Data from Power Plant). Similar Biomass feedstock was characterized previously in the scope of project *Bias-to-Soil* (PTDC/AAC-AMB/098112/2008) also developed at LNEG. The characterization was made over samples collected during a year and the mean values and range are summarized in **Table 5.**

Table 5 - Biomass characterization from FB Industrial Unit (adapted from Lopes (2013))

(LHV – Low Heating Value d.b. - dry basis; wt% - weight percentage)

	Method	Average	Min	Max
LHV (MJ/kg)	CEN/TS 15400	18,4	17,4	19,4
Proximate Analysis (d.b., wt%)				
Ash	CEN/TS 14775	7,2	4,2	10,6
Volatile Matter	CEN/TS 14918	74,0	72,0	76,2
Fixed Carbon	Calculation	18,8	17,4	20,5

	Method	Average	Min	Max
Elemental Analysis (d.b., wt%)				
C	CEN/TS 15104	51,2	47,7	54,1
H	CEN/TS 15104	5,4	5,1	5,6
N	CEN/TS 15104	0,4	0,3	0,4
S	CEN/TS 15289	0,12	0,08	0,16
O + Error	Calculation	35,9	34,7	37,0
Cl Soluble	CEN/TS 15105	0,11	0,10	0,12
Minor Elements (d.b., mg/kg)				
Cd	EN 13656	<0,25	-	-
Cu		8	6	11
Cr		42	28	58
Mn		224	145	321
Ni		25	17	36
Pb		3	2	6
Zn		24	17	37
Hg	ASTM D 6722-01	0,019	0,012	0,026
Major Elements (d.b. wt%)				
Al	ASTM D 3682	0,33	0,15	0,70
Ca		0,94	0,71	1,56
Fe		0,16	0,08	0,32
K		0,35	0,28	0,47
Mg		0,13	0,12	0,16
Na		0,20	0,13	0,32
Si		1,36	0,59	2,44
Ti		0,009	0,003	0,020
P	EN 13656	0,12	0,08	0,18

The characteristics of this biomass mixture fluctuate along time, depending on the year period. Principal concerns, regarding this fuel, are related with the high moisture content, in the range of 40 % to 55 % (wt%, w.b.), and the high content of exogenous inert material – soil and stones – up to 20 % (wt%, d.b.), implying a frequent bottom bed discharge to maintain the bed height of the FB combustor (Tarelho *et al.*, 2014).

The ash amount in this fuel has a wide range of variation from 4,2 % to a considerably-high 10,6 % when compared to the reference biomass compositions in Table 2 in Section 1.1.2. The reference woody biomasses vary their ash content between 0,3 % to 2,0 % while the herbaceous, straw and grass, account for 5 % and 7 %, respectively. This high ash content may be a result of the presence of soil particles in the fuel.

Chlorine share is ten times higher than the reference woody biomass, which may be a result of the incorporation of leaves and needles, from the forest biomass residue produced in Portugal.

Calcium presents a high share in this fuels 0,72 % to 1,6 %, and a higher share when compared with the reference biomasses: 0,09 % to 0,5 % (wood and residues/bark, respectively). Since calcium is an important element in both S and Cl retention, the following molar ratios were determined considering the average concentrations from **Table 5**: n_{Ca}/n_S of 6,3; n_{Ca}/n_{Cl} of 7,6 and $n_{Ca}/n_{(S+Cl)}$ of 3,4. From these molar ratios it is expected that S and Cl will be retained by calcium presented in the fuel, thus minimizing SO_2 and HCl emissions in the stack.

Also, sodium presents high share between 0,13 % to 0,32 % against a 0,002 % to 0,1 % (wood and grass, respectively) share of the reference. On the other hand, potassium share is inside the reference range.

Silicon share presents a wide range from 0,6 % to 2,44 % which is much higher than the referenced range of 0,02 % to 1,5 % (wood and grass, respectively). This may be a consequence of soil presence in the biomass feedstock.

Regarding heavy metals, and focusing on lead, copper and zinc shares, overall this biomass has similar concentration than the reference biomasses:

Copper (Cu) share has the biggest gap from the references, with 6 mg/kg to 11 mg/kg against 2 mg/kg to 5 mg/kg (of wood/straw and bark/grass, respectively);

Lead (Pb) is in the referee range with 2 mg/kg to 6 mg/kg against 0,5 mg/kg to 4 mg/kg (straw and bark, respectively);

Zinc (Zn) presents a wide range from 17 mg/kg to 37 mg/kg while the reference biomass present from 10 mg/kg to100 mg/kg, for wood/straw, grass and bark, respectively.

2.3 FLUE GAS CHARACTERIZATION

In this study, the characterization *in situ* was developed at the industrial partner installation, with both continuous and discontinuous sampling processes. The continuous process, where flue gas sampling is performed by automatic equipment, was used for the CO, CO_2, O_2, SO_2 and NO_x parameters. The discontinuous processes, defined as the sample extraction with manual equipment, was used for the Total Suspended Particles (TSP), chlorinated compounds (HX), Particulate Granulometric Classification (PGC) and Particulate Matter ($PM_{10/2,5}$) parameters determination.

The methods and technics applied in the determination of stack-gas emissions from combustion, should be, and by order of priority, CEN (*Comité Européen de Normalisation*) European standards (EN), ISO (International Organization for Standardization) or other national or international recognized methodologies could be used, such as the U.S. Environmental Protection Agency methods (EPA) (IED, 2010). Portuguese Standard (NP) were also used when possible.

For PGC sampling was done according to the *Mark III User Manual* (Eight-stage Cascade Impactor ANDERSEN Mark III Particle Sizing), which is based on EPA methods. While TSP and $PM_{10}/PM_{2,5}$ were sampled according to EN and ISO methods. Used methods are summarized in **Table 6**

Table 6 – Flue gas sampling methods

Parameter	Method	
	EN/ISO	EPA
Sampling area location	-	Method 1
Sampling points	NP EN 13284-1:2009	Method 1
Velocity and volume flow rate	EN ISO 16911-1:2013	Method 2
Molecular weight	-	Method 3
CO_2, O_2	-	Method 3A
SO_2	-	Method 6C
NO_x	-	Method 7E
CO	-	Method 10
Moisture	EN 14790:2005	Method 4
TSP	EN 13284-1:2009	-
PGC	-	Method 5
HCl emissions	Internal Method HCl	-
$PM_{10}/PM_{2,5}$	EN ISO 23210:2009	-

The procedures used for the sampling of the parameters mentioned in **Table 6** are described in the following sections, from **2.3.1** to **2.3.10**. Some parameters rely on the prior sampling and determination of other parameters so, in order to understand the order of parameters determined during sampling, a scheme of the parameters dependence is presented in **Figure 8**. Also, the equations taken from the sampling methodologies and used in the analytical determination of the parameters are summarized in **Table 7**.

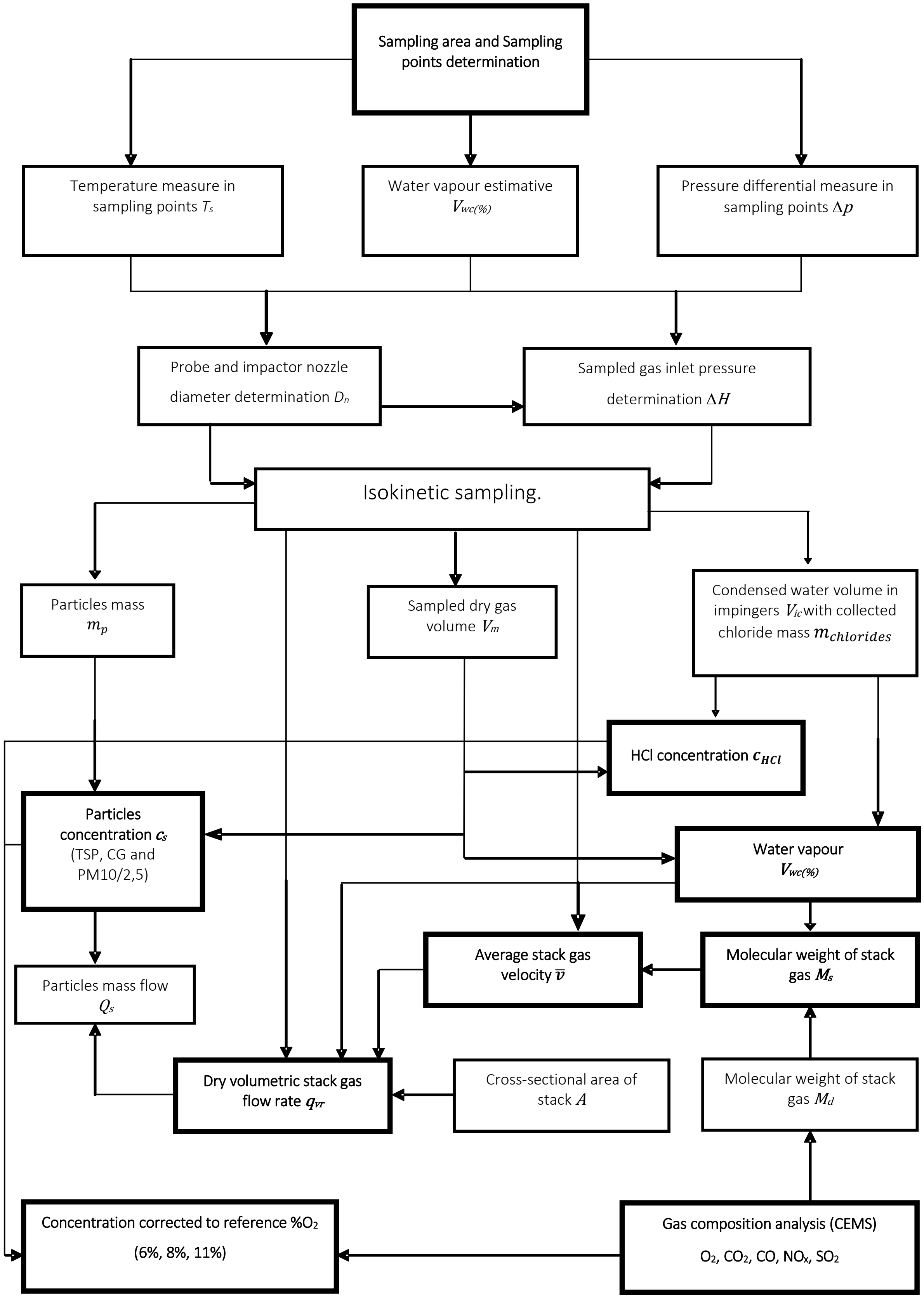

Figure 8 – Schematic representation of the flue gas characterization procedure

Table 7 *– Equations used for stack sampling*

Parameter	Method			
	EN/ISO		EPA	
Flue gas velocity	$\bar{v} = KC\sqrt{\frac{T_s\Delta\bar{p}}{p_e M_s}}$	Eq. (2a)	$v_s = K_p C_p\left(\sqrt{\Delta P}\right)_{avg}\sqrt{\frac{(T_s)_{avg}}{P_s M_s}}$	Eq. (2b)
Volumetric flow rate	$q_{vr} = \bar{v}A\left(\frac{273}{T_s}\right)\left(\frac{p_e}{101,3}\right)$	Eq. (3a)	$Q_{sd} = 3600(1 - B_{ws})v_s A_s\left[\frac{T_{std}P_s}{(T_s)_{avg}P_{std}}\right]$	Eq. (3b)
Molecular weight	$M_s = 29$ kg/kmol		$M_s = M_d(1 - B_{ws}) + 18B_{ws}$	Eq. (4)
			$M_d = 0{,}44(\%CO_2) + 0{,}32(\%O_2) + 0{,}28(\%N_2 + \%CO)$	Eq. (5)
Dry gas sampled	$V_{m(std)} = (V_2 - V_1)\frac{T_{std}}{T_m}\frac{p_m}{p_{std}}$	Eq. (6a)	$V_{m(std)} = V_m\,Y\left(\frac{T_{std}}{T_m}\right)\left(\frac{P_{bar} + \frac{\Delta H}{13,6}}{P_{std}}\right)$	Eq. (6b)
Moisture	$V_{wc(g/m^3)} = \frac{m_{wc}}{V_{m(std)}}$	Eq. (7a)	$V_{w(std)} = \frac{V_{ic}\,\rho_w\,R\,T_{std}}{M_w\,P_{std}}$	Eq. (7b)
	$V_{wc(\%)} = \frac{\frac{m_{wc}V_{mol(std)}}{M_w}}{\frac{m_{wc}V_{mol(std)}}{M_w} + V_{m(std)}} \times 100$	Eq. (8a)	$B_{ws} = \frac{V_{w(std)}}{V_{m(std)} + V_{w(std)}}$	Eq. (8b)
Isokinetic	$I = \frac{v_N}{v_a}$	Eq. (9a)	$I = \frac{100T_s\left[K_4V_{ic} + \left(V_m\frac{Y}{T_m}\right)\left(P_{bar} + \frac{\Delta H}{13,6}\right)\right]}{60\theta v_s P_s A_n}$	Eq.(9b)
Particle concentration	$c_s = \frac{m_p}{V_{m(std)}}$			Eq. (10)
Particles mass flow	$Q_s = c_s Q_{sd}$			Eq. (11)
HCl emissions	$C_{chlorides\,(HCl)} = \frac{m_{chlorides}}{V_{m(std)}} \times \frac{M_{HCl}}{M_{Cl}}$			Eq. (12)
Concentration in reference %O$_2$	$C_{ref} = C_{avg} \times \frac{21 - O_{2\,ref}}{21 - O_{2\,avg}}$			Eq. (13)

2.3.1 SAMPLING AREA LOCATION

The location of the sampling points was determined according with methods presented in the Manual of the Cascade Impactor, based on the EPA Method 1 *Sample and Velocity Traverses for Stationary Sources*.

The sampling points are located in a cross section normal to the axis of the duct at the sampling position. It shall be as far downstream and upstream from any disturbance, avoiding changes of direction in the flue gas flow. Therefore, leads to a height equal to, at least, eight internal diameters upstream and five downstream of flow disturbance.

For the experimental facility tested, the stack presented an internal duct diameter of 1,4 m, theoretically leading to x_1= 11,2 m and x_2= 7 m. Hence, the sampling section of the industrial unit´s stack, located 20 m above the stack base, obeys the standard criteria, and is shown in **Figure 9**.

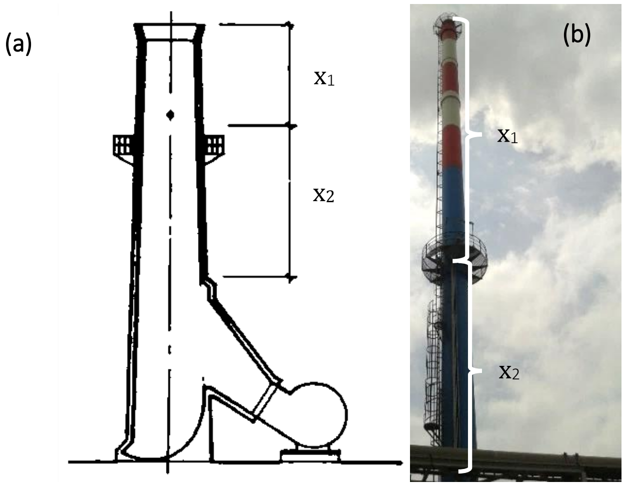

Figure 9 – Sampling area location: (a) Schematic representation, (b) On site location

All the sample material and equipment necessary to carry out the stack-gas samplings were raised to the measuring site through a cable and sheave, as shown in **Figure 10.**

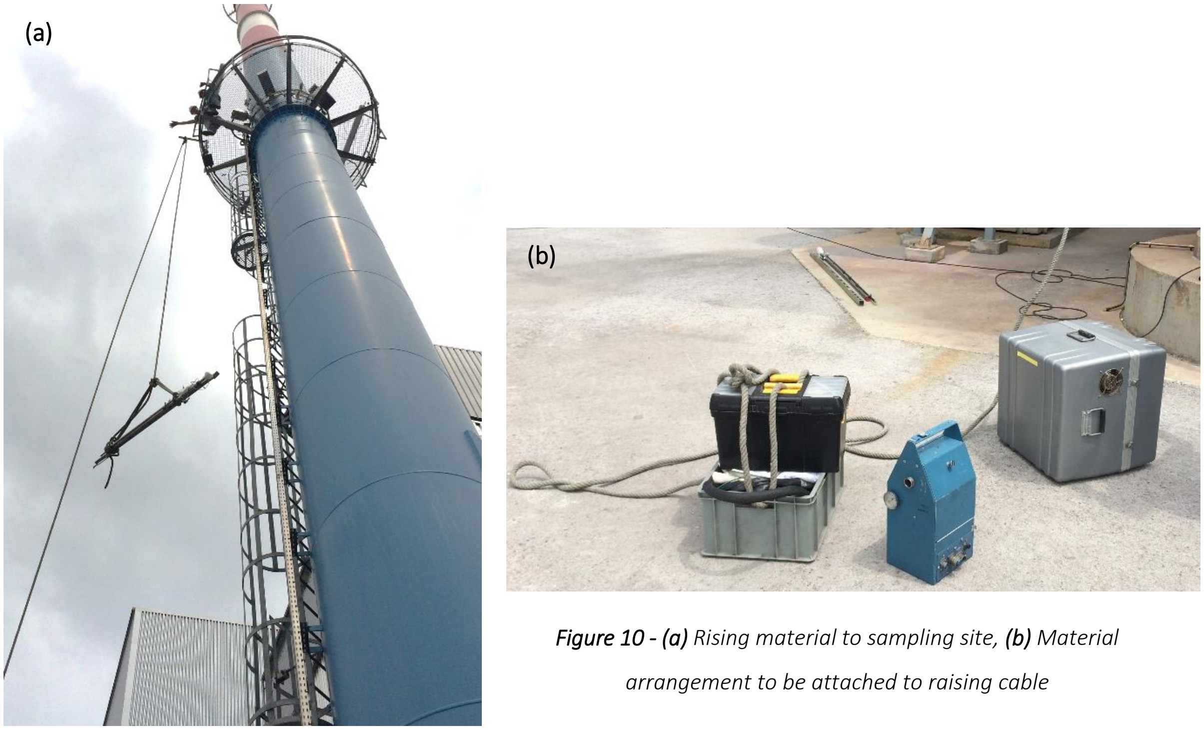

*Figure 10 - **(a)** Rising material to sampling site, **(b)** Material arrangement to be attached to raising cable*

2.3.2 SAMPLING POINTS

Sampling points amount was determined by both methodologies: *a)* NP EN 13284-1:2009 *Stationary source emissions - Determination of low range mass concentration of dust - Part 1: Manual gravimetric method* (for TSP and $PM_{10}/PM_{2,5}$ sampling), and; *b)* EPA Method 1 *Sample and Velocity Traverses for Stationary Sources* (for PGC sampling).

Flue gas velocity and particle flow can only be sampled in discrete points, which leads to a need of a representative point localization inside the duct.

Due to standard restrictions related to the stack's internal diameter – 1,4 m – the minimum number of points were: *a)* four points determined by the EN Standard, and; *b)* six points by the EPA method. Sampling point distances, from the access port entrance, are summarized in **Table 8**, and schematically represented in **Figure 11**.

Table 8 – Stack sampling points distance from access port

Sampling Point	EN (m)	EPA (m)
p_1	0,34	0,31
p_2	0,60	0,45
p_3	1,30	0,66
p_4	1,56	1,24
p_5		1,45
p_6		1,59

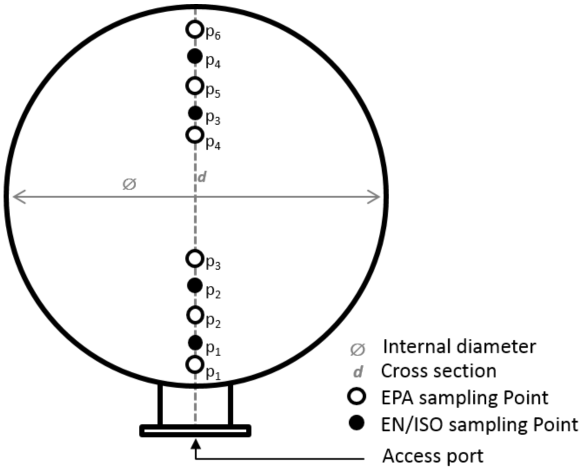

Figure 11 *- Stack sampling points location inside the stack, schematic representation*

The sampling line length is a sum of the internal diameter of the stack with the access port length (0,25 m).

Although the standards implies the use of two sampling lines with 90° difference between them, for the purpose of the present study and due to time constraints at the sampling location, the isokinetic samplings were carried out only using one sampling line.

2.3.3 CO, CO_2, O_2, SO_2, NO_X ANALYSIS

The analysis of these gases was done according to the EPA methods 3A, 6C, 7E and 10, using an TESTO 350 analyser with an electrochemical cell as the measuring principle.

The TESTO 350 analyser was used as support measurement. This analyser was calibrated for the analysed gases and verification was periodically carried out, with certified gas mixtures of 4,96 O_2, 12,01 and 16,0% CO_2, 500,4 and 4000 ppm CO, 384 ppm NO and 404ppm SO_2.

The gases were also analysed by the PP's Continuous Emissions Monitoring System (CEMS) equipment, simultaneously with the other parameters. This equipment is an Advance Optima AO2040, with an infrared analyser module Uras26. Its measurement principle consists in a non-dispersive infrared (NDIR) absorption in the λ = 2,5 to 8 µm wavelength range.

The data obtained was converted to the reference oxygen (6%, 8%, 11%) used in the ELV regulations, by **Eq. (13)**, from **Table 7**. This conversion was also applied to other measured parameters: TSP, PGC and $PM_{10/2,5.}$

2.3.4 VELOCITY AND VOLUMETRIC FLOW RATE OF FLUE GAS

Flue gas average velocity and volumetric flow rate were determined according to the methodologies: *a)* ISO 16911-1:2013 *Stationary source emissions – Manual and automatic determination of velocity and volume flow rate in ducts – Part 1: Manual reference method*, and; *b)* EPA Method 2 - *Determination of Stack Gas Velocity and Volumetric Flow Rate (Type S Pitot Tube)*.

These methodologies consist in measuring the temperature, static pressure and the differential pressure of the flue gas with the S-type pitot tube and thermocouple on the sampling probe, of the sampling train, in each sampling point. These values are also important for the determination of nozzle diameter, to be used during particulate sampling. Both the pitot tube and the thermocouple were calibrated.

The sampling train scheme is presented in **Figure 12**.

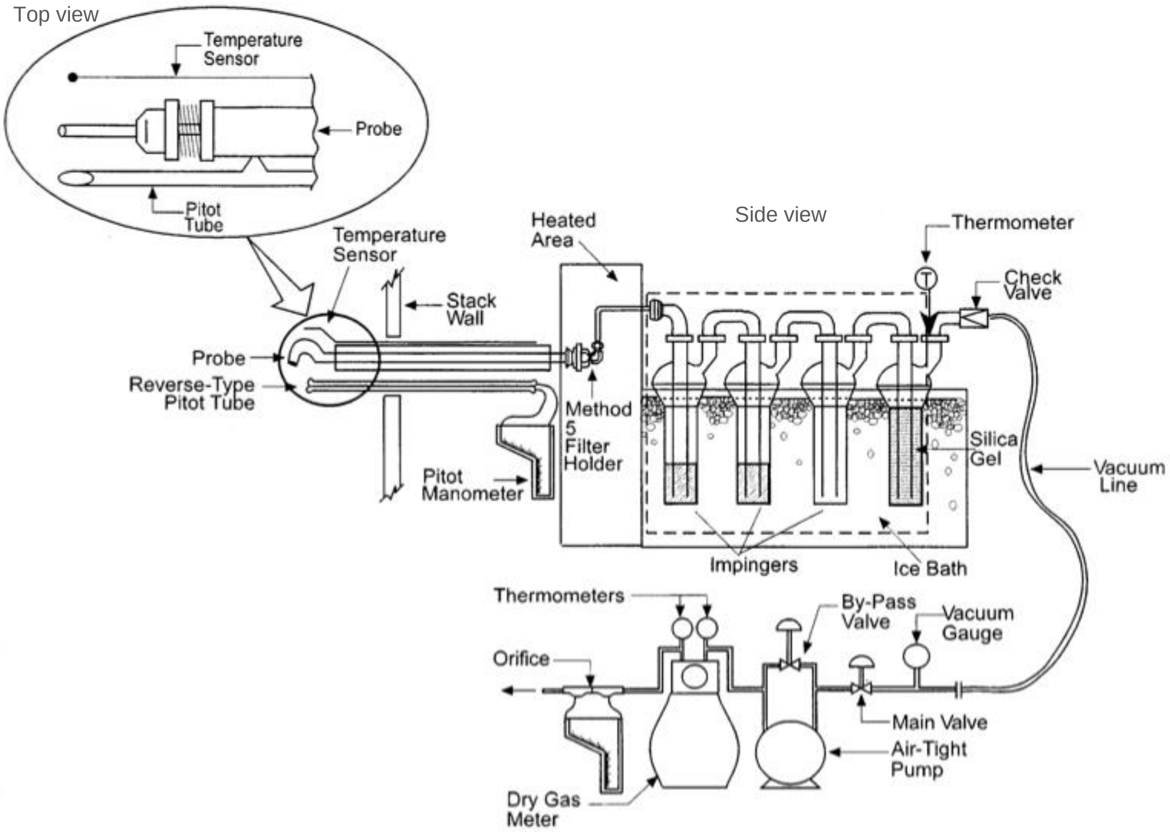

Figure 12 - *Sampling train schematic representation (adapted from (EPA5))*

A picture of the sampling train equipment used was a Baldwin Environmental Equipment, Inc (BEI) Model 32, shown in **Figure 13**.

Figure 13 – *Sampling train: (a) 1 Probe, 2 Heated area, 3 Ice bath, 4 Umbilical cord (b) Control Unit*

This equipment is conceived and operated to avoid condensation, chemical reactions and to minimize particle deposition upstream of the filter and not to have leaks along the sampling train. Condensation is avoided by heating the train from probe to the Heated Area. The gas is then cooled and adsorbed in the Ice Bath which holds four impingers. The volume of sampled gas is regulated by a Control Unit, which follows the Ice Bath, by means of an Umbilical Cord. The control unit allows to adjust gas flow and temperature control, by means of adjusting valves.

Using the average value for each mentioned variable along with the molecular weight and gas moisture, the average velocity and the average flow rate of dry gas was obtained by **Eq. (2a)**, **Eq. (3a)** for the EN standards and **Eq. (2b), Eq. (**. (3b**)** for the EPA Methods, from **Table 7**.

2.3.5 MOLECULAR WEIGHT

The concentration of N_2 and the molecular weight of the other gases, in dry basis, were determined using the methods based on the EPA Method 3 - *Gas Analysis for the Determination of Dry Molecular Weight*.

Values were obtained using the concentration results from **Section 2.3.3**, **Eq. (4)** and **Eq. (5)** from **Table 7,** for EPA Methods.

For the sampling tests that followed the EN standards, the molecular weight of stack gas (M_s) is considered to be 29 kg/kmol, for molecular masses between 27 kg/kmol and 31 kg/kmol.

2.3.6 MOISTURE

Flue gas moisture was determined by the EN 14790:2005 *Stationary source emissions – Determination of the water vapour in duct*, by the methods presented in the Manual of the Cascade Impactor, based on the EPA Method 4 - *Determination of moisture content in stack gases*.

A gas sample is extracted at a constant rate from the stack with the sampling train. The water vapour of that sample is subsequently trapped by condensation plus adsorption inside impingers; the mass of water is then determined by weighing the mass gain of the trapping unit. This trapping unit, referred to as Ice Bath, consists in four ice-cooled impingers: two with deionized distilled water, one empty and one with silica gel, as shown in **Figure 12**.

Respectively, the dry gas volume sampled from the gas meter at standard conditions, the volume of water vapour collected in standardized conditions and the water vapour content, are given by **Eq.(6a)**,

Eq.(7a) and **Eq.(8a)** , from **Table 7**, for EN standard while **Eq.(6b)**, **Eq.(7b)** and **Eq. (8b)** were used for EPA Methods.

2.3.7 TOTAL SUSPENDED PARTICLES

Total Suspended Particles (TSP) emissions were determined by the method described in NP EN 13284-1:2009 *Stationary source emissions - Determination of low range mass concentration of dust – Part 1: Manual gravimetric method*.

This method implies the determination parameters previously mentioned, as summarized in **Figure 8**. TSP samples were extracted with the sampling train, **Figure 12**, under isokinetic conditions.

Isokinetic sampling consists in flue gas sample extraction at such flow rate that the velocity and the direction of the gas entering the sampling nozzle (V1) are the same as in the duct (V2), **Figure 14** presents a schematic representation of flue gas sampling conditions.

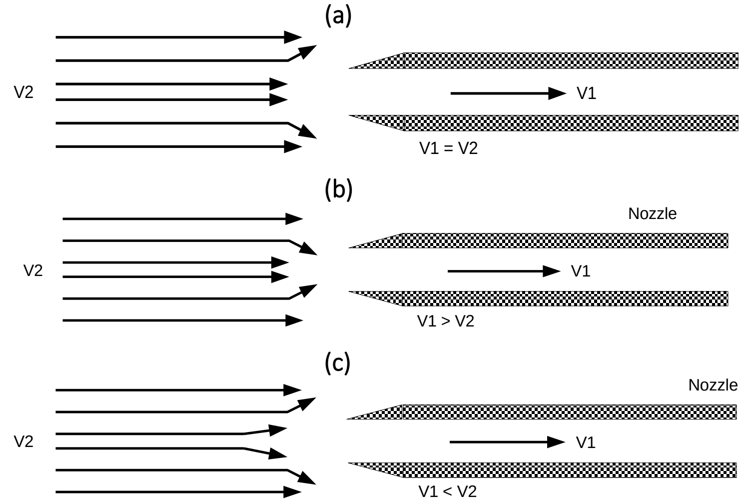

Figure 14 *– Flue gas sampling schematic representation: (a) isokinetic, (b) over-isokinetic, (c) under-isokinetic*

The sampling validation is given by the isokinetic factor (I), **Eq.(9a)** and **Eq.(9b)** for EN and EPA Methods respectively. TSP sampling is valid with isokinetic range: 95 % < I < 115 %.

Particles separation from the gas is done by a pre-weighted glass fibre plane filter, which is dried post-sampling and re-weighted, according to the following procedure:

1) Pre-sampling: Filters must be dried during at least 1 h, in an oven at a minimum of 180 °C;
2) Leave the filters to cool down at room temperature inside a desiccator, for at least 4 h,

3) Post-sampling: Filters must be dried during at least 1 h, in an oven at a minimum of 160 ^{0}C;
4) Filters cool down as described in step *2)*;
5) Filters weighting must be done in the 3 min that follow the filter removal from the desiccator. Three weight readings must be done at 1 min, at 2 min and at 3 min. If a relevant increase is detected repeat step *4)*. The reference dry weight is then determined by extrapolation to minute zero.

Particles concentration in flue gas (mg/Nm^3) and their mass flow (kg/h) are then determined, with the weighted particle mass collected divided by sampled dry gas volume, by **Eq.(10)** and **Eq.(11)** from **Table 7**.

2.3.8 PARTICULATE GRANULOMETRIC CLASSIFICATION

Particulate Granulometric Classification (PGC) requires sampling of particles following a method based on EPA Method 5 - *Determination of particulate matter emissions from stationary sources*.

This method is based in isokinetic sampling, between 90 % < I< 110 %. Using the sampling train, the particles are separated into eight classes of aerodynamic diameter and collected on glass fibre filters of each stage, located inside the cascade impactor. Each stage is constituted by a filter and its support plate. Particles mass collected in each filter are determined gravimetrically after sampling.

The equipment used was an eight-stage cascade impactor *Mark III Particle Sizing Stack Sampler – Andersen*, **Figure 15**, attached to the sampling probe of the sampling train as represented in **Figure 16**.

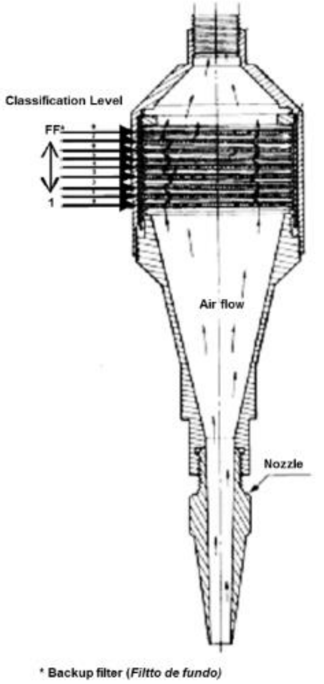

__Figure 15__ – Mark III impactor, schematic representation (adapted from Salema (2008))

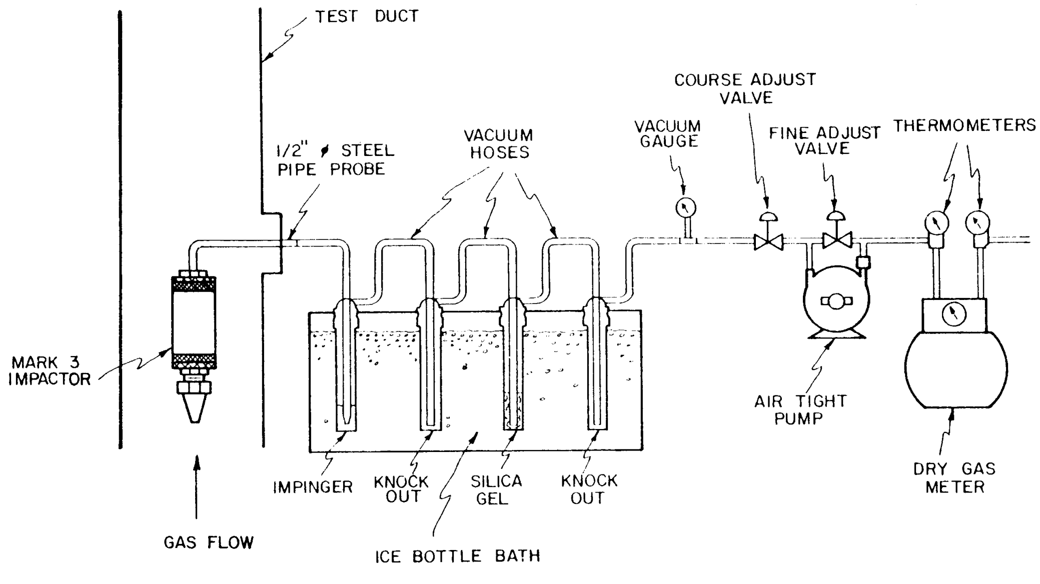

__Figure 16__ - Mark III attached to the sampling train, schematic representation (adapted from the MARK III User Manual)

Aerodynamic diameter equals the diameter of a sphere with a particle unit-mass density of 1 g/m^3, under the same external conditions. The mechanism of separation is called impaction: the aerosol collected by the nozzle is accelerated to pass through the holes of each of the eight internal plates and then deflected by 90°, due to the configuration of stack plates' assembly.

Particles with greater aerodynamic diameter are not able to follow the gas flow due to their mass inertia. Hence, the sampled gas flow, alongside with the stack temperature during sampling, define the cut-off diameter for each plate. The *Mark III User Manual* presents charts of the aerodynamic diameter (µm) variation as a function of the flue gas flow (acfm), for various stack temperatures (F) ranges. Therefore, it is possible, given a temperature and flue gas flow, to determine the aerodynamic diameter for each stage of the *Mark III*.

The impacted particles on the filter of a plate/stage, as shown by **Figure 17**, defined by a cut-off diameter d_{50}, *i.e.*, for particles with a specific aerodynamic diameter, the separation efficiency of that stage is 50 %.

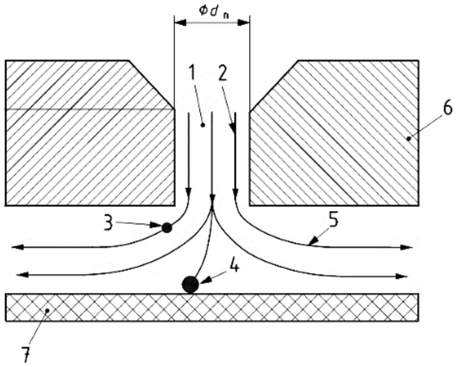

1 – Internal plate hole
2 – Flow line
3 – Particle remaining in the flow
4 – Impacted particle
5 – Particle trajectory
6 – Internal plate
7 – Collecting stage
$\varnothing d_n$ – Plate hole inlet

Figure 17 *– Principle of impaction (adapted from NPISO23210 (2009))*

The particles are collected as a function of decreasing inertia, hence samples of decreasing aerodynamic particle size are obtained stage by stage, in direction of flow towards the last plate. The particles not retained by any of the stages are collected in a backup filter downstream of the impactor stages. Filters of quartz fibre are used to retain particles in each plate/stage.

The samples were weighted, according to the procedure described in **Section 2.3.7**. A frequency distribution in function of particle aerodynamic diameter, as well as a cumulative frequency were developed. The cumulative frequency allows the determination of the diameter, below of which correspond 50 % of the total particle mass.

2.3.9 $PM_{10/2,5}$

The aerodynamic diameter classification of particles present in the flue gas proceeded under the *Stationary source emissions - Determination of PM10/PM2,5 mass concentration in flue gas – Measurement at low concentrations by use of impactors*.

This method is based on the previously mentioned principle of Impaction, with a constant flue gas sample volumetric flow rate. Sampling is representative of the stack flue gas if the isokinetic rate is between 90 % and 130 %, if isokinetic sampling is impossible, over-isokinetic sampling is preferred, as represented in **Figure 14 (b)**.

A two-stage cascade impactor Stainless steel Impactor TECORA MSSI was used for this parameter, **Figure 18**, attached to the probe from the sampling train represented in **Figure 19**.

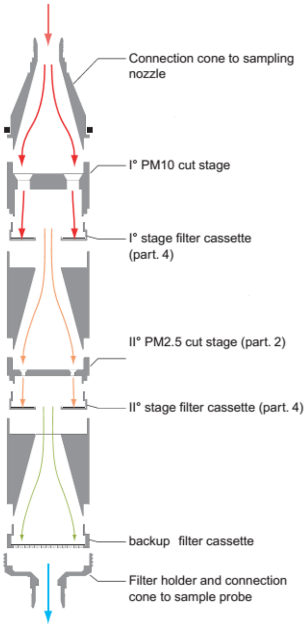

Figure 18 – *TECORA MSSI impactor, schematic representation (adapted from TECORA (2015))*

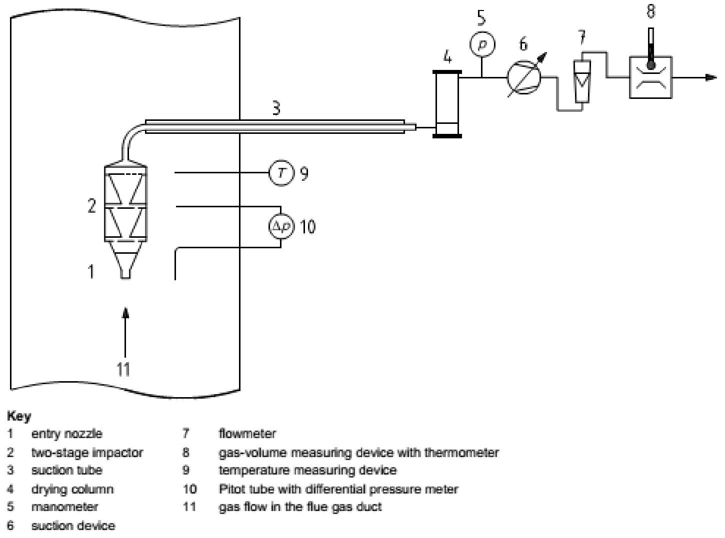

Figure 19 - TECORA MSSI attached to sampling train, schematic representation (adapted from (NPISO23210, 2009))

During sampling, the particles carried with the flue gas are divided into three groups according to aerodynamic diameters, defined by each impactor stage:

- First stage: particles greater than 10 µm;
- Second stage: particles between 10 µm and 2,5 µm;
- Backup filter: particles smaller than 2,5 µm.

Therefore, $PM_{2,5}$ mass corresponds to the fraction collected in the backup filter and PM_{10} corresponds to the mass collected in both the second impactor stage and backup filter. Filters used are pre and post-sampling weighted, according to the procedure described in **Section 2.3.7**, in order to determinate the collected particles concentration.

As previously explained (**Section 2.3.8**), the cut-off diameter depends on the flue gas flow and stack temperature. Therefore, and in order to achieve the specific cut-off diameters of 10 µm and 2,5 µm on the first and second stage, respectively, the ideal flue gas flow is determined previously to the sample, in order to the flue gas velocity inside the stack.

In order to avoid moisture condensation inside the impactors, both systems – Mark III and TECORA MSSI - were externally heated with a heating mantle at around 160 ^{o}C, **Figure 20.**

Figure 20 – *Impactors: (1) TECORA MSSI, (2) Mark III*

2.3.10 HCl EMISSIONS

For determination of hydrogen chloride (HCl), flue gas was sampled using a LNEG Internal Method based in the European standard EN 1911 - *Stationary source emissions* - *Determination of mass concentration of gaseous chlorides expressed as HCl – Standard reference method.*

Simultaneously, flue gas sample for this method were extracted for TSP, PGC and $PM_{10/02,5}$ sampling. After the particulate matter collection in the filters, the HCl in the flue gas sampled is collected in the impinger's deionized distilled water, by condensation.

HCl was measured in the collected solutions from the impingers, through ionic chromatography analysis, after a pre and post-weighting of the impingers. The concentration of HCl in the collected solution is given by **Eq.(**12**)**, from **Table 7**.

2.4 SAMPLING PERIODS

Several sampling periods were performed during two days (Day A and Day B), comprising sampling for TSP, PGC and $PM_{10/2,5}$.

Two samples of Total Suspended Particle were performed in both days and the codification attributed is TSPA and TSPB (respectively, day A and B). The $PM_{10/2,5}$ sampling performed in day A is given the codification PMA, while the Particulate Granulometric Classification the codification is PGCA.

Simultaneously during TSPA, TSPB, PMA and PGCA the HCl samplings were carried out. **Table 9** summarizes all this information.

***Table 9 –** Sample's nomenclature*

Nomenclature	Parameters	Day	Hour
TSPA	TSP	A	12:56 – 15:56
HClA1	HCl+ Moisture		
PMA	$PM_{10/2,5}$		17:51 – 19:51
PGCA	GC		19:58 – 21:10
HClA2	HCl + Moisture		17:51 – 21:10
TSPB	TSP	B	13:05 – 15:05
HClB	HCl + Moisture		

Sample filter codifications for $PM_{10/2,5}$ and PGC were attributed by the flow´s upstream-downstream direction, inside the impactor. Hence, the A series of each parameter defined as:

For $PM_{10/2,5}$: PMA_1 (> 10 µm), PMA_2 (2,5 µm > PMA_2 < 10 µm), PMA_F (< 2,5 µm);

For PGC: PGCA_1, PGCA_2, PGCA_3, PGCA_4, PGCA_5, PGCA_6, PGCA_7, PGCA_8, PGCA_F.

2.5 POWER PLANT OPERATION

The combustion performance during the sampling periods was analysed through the freeboard zone gas temperature (Data from PP). The working regime of the particles cleaning system was analysed through the voltage of the ESP's third field. The temperatures and voltage profiles are presented in **Figure 21**, for day A and B.

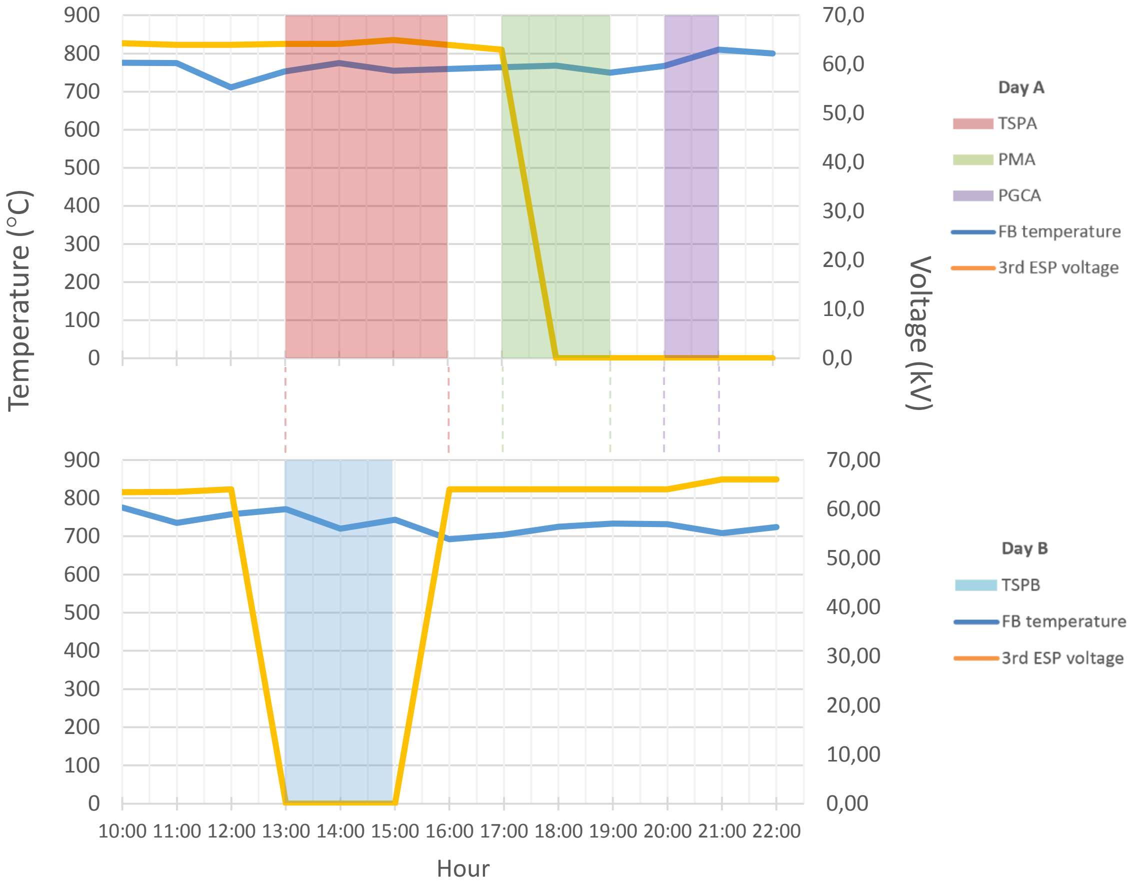

***Figure 21** – FB temperature and ESP voltage profiles during sampling periods*

The boiler temperature profile was kept between the range of 700 °C and 800 °C, with a daily average of 760,9 °C and 743,3 °C on day A and B, respectively. Hence, it means that the combustion was occurring under steady state operation, which is a useful information to understand the emissions sampled and registered during the sampling periods. Also the bed temperatures presented a variation of 870 °C ± 20 °C for the two days.

Regarding the third field of the ESP, it shows a null voltage from 18:00 h (around middle of PMA sampling) until the end of the sampling periods on day A and during the total sampling period day B, from 13:00 h to 16:00 h. The ESP was partially shut down during these periods, only the third field was turned off, overall it was working at 66 % of its capacity. This happened in a cooperation agreement with the Industrial PP, since the purpose of the project was to study the composition of the produced fly-ash particles and not to quantify its atmospheric emissions, which are controlled under efficient flue gas treatment with the ESP working properly.

2.6 PARTICLES CHARACTERIZATION

The filters with the collected particles were morphologically characterized, after the quantification procedures. A Stereomicroscope, Olympus SZH with an Olympus DP20 Digital Camera coupled, was used to observe the overall particles collected in the filters.

An Electron Microprobe JEOL JXA 8500F, **Figure 22**, was used to provide information about sample composition and morphology, by means of Electron Dispersive Spectroscopy (EDS) and Wavelength Dispersive Spectrometry (WDS).

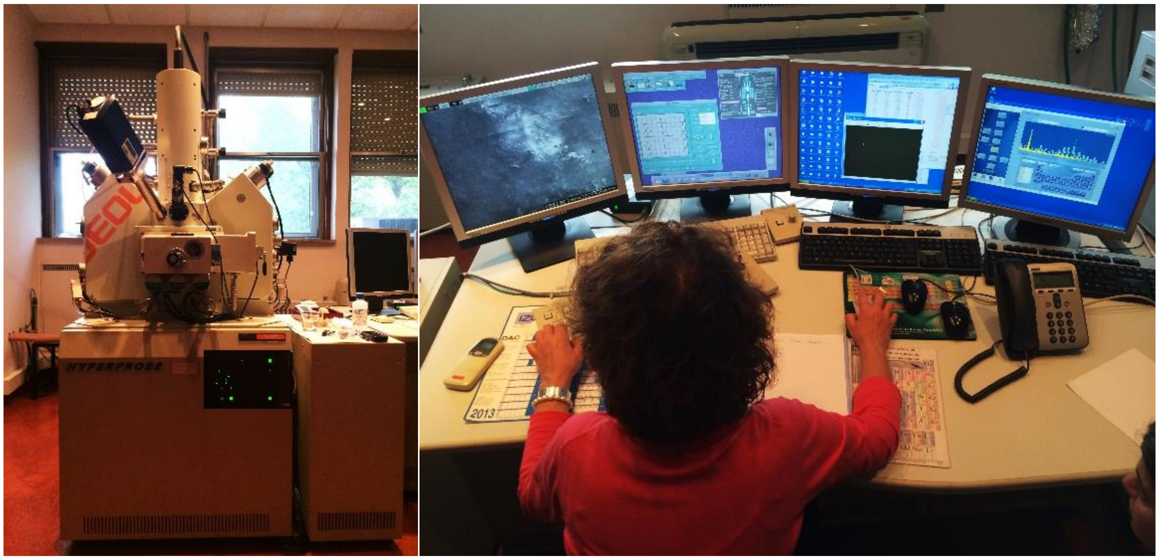

Figure 22 *– Scanning Electron Microscopy equipment (JXA-8500F)*

The heart of the JXA-8500F is effectively a Scanning Electron Microscopy (SEM) column, in which an electron emitter, or field-emission gun, bombards the specimen with a beam of electrons. When the electron beam hits the specimen, some electrons are scattered and some are absorbed. Scattered electrons are detected and converted into images that provide information about sample composition and surface morphology by contrast. Also, heavier elements will appear brighter than lighter elements, due to different atomic numbers. The hole left by the scattered electron is then filled by a higher level electron, releasing an X-ray by moving from one higher energy layer to a lower one. EDS provides a spectrum (number of X-rays detected by energy level in keV) of the scanned point/area from where it is possible to observe the elemental relative proportions.

Samples must be vacuum-stable and conductive for a SEM analysis, hence samples of several fragments of the filters, containing particles, were prepared in a BAL-TEC SCD 005 Cool Sputter

Coater. The samples, fixed to a metallic support, were put inside a vacuum chamber, in the assemblies shown in **Figure 23**, where they were sputter-coated with a carbon film, allowing the sample to be electrically conductive.

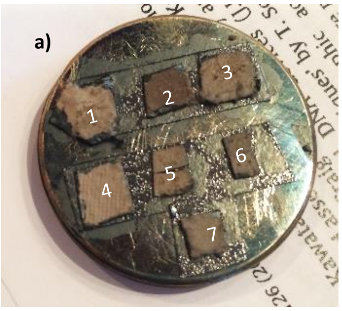

1 – PMA_2
2 – PMA_F
3 – PMA_1
4 – TSPA
5 – PGCA_3
6 – PGCA_6
7 – PGCA_F

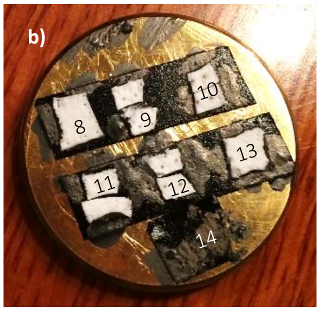

8 – PGCA_F
9 – PGCA_8
10 – PGCA_5
11 – PGCA_1
12 – PGCA_7
13 – TSPB
14 – Pyramid (PMA_2)

Figure 23 – *Samples assembly for SEM analysis*

In assembly **a)**, samples had already been through the sputter-coating process, justifying the darker colour of the samples (1 to 7) when compared to the samples before coating in assembly **b)** (8 to 14).

3 RESULTS & DISCUSSION

3.1 EMISSIONS CHARACTERIZATION

During the sampling periods the flue gas was analysed for O_2, CO, CO_2, NO_x and SO_2 concentrations (**Section 2.3.3**), HCl concentration (**Section 2.3.10**) and moisture content concentration (**Section 2.3.6**).

The average results for each sampling period are summarized in **Table 10.**

Table 10 – Flue gas O_2, CO_2, CO, NO_x, SO_2, HCl and moisture concentrations, and other measured parameters

	O_2	CO_2	CO	NO_x	SO_2	HCl	Gas moisture	Gas temperature	Gas velocity	Dry gas flow
	(%)		(mg/Nm^3, 6%O_2)			(mg/Nm^3, 10%O_2)	(%)	(°C)	(m/s)	(Nm3/h)
TSPA / HClA1	9,4	11,1	236	339	53	31	11,1	142	28,3	9,1 x 10^4
TSPB / HClB	9,2	11,2	330	328	58	28	11,1	138	24,8	7,8 x 10^4
PMA	9,3	11,1	263	352	68	41	10,7	140	27,9	8,7 x 10^4
PGCA	9,4	11,0	384	354	93			144	28,0	1,0 x 10^5
HClA2	9,4	11,0	316	352	80	41	10,7	142	28,0	9,3 x 10^4
Daily average										
Day A	9,3	-	278	336	74					
Day B	9,2	-	322	325	68					

Although HCl emissions are not legislated for combustion system using biomass as fuel, and using the value 10 mg/Nm^3 (at 10% O_2) as reference for the waste incineration plants of the IED and 25,4 mg/Nm^3 (at 10% O_2) from general ELV from the Portuguese Decree-Law 78/2004, relevant concentrations of HCl were collected for three samples: 28 mg/Nm^3, 31 mg/Nm^3 and 41 mg/Nm^3 (at 10% O_2, dry gas).

SO_2 and NO_x emissions values were below the ELV proposed in the new MCP directive, presented in **Table 3**. Also, these values are below the maximum theoretical emissions determined, as presented in **Table 11.**

Theoretical concentrations emissions, at the stack, were determined considering the combustion reaction, **Reaction (1)**, an excess air in the stack $\%\boldsymbol{e_{air}} =$ 79 % determine by **Equation (1)**,and using the fuel characterization from **Table 5** with an average moisture content of 47,5 % (wt%, w.b.).

Table 11 *– Maximum theoretical gaseous and HCl emissions, and flue gas moisture*

O_2	CO_2	NO_x	SO_2	HCl	Gas moisture
(%)		(mg/Nm^3, 6%O_2)		(mg/Nm^3, 10%O_2)	(%)
9,3	11,1	1955	680	124	20,0

The values measured at the stack are considerably lower than maximum theoretical values. This gap accounts for the emissions retained in the system, due to the primary emission reduction measures: air staging (reducing NO_x emissions) and interactions with bed material and fuel ashes (retaining the SO_2 and HCl emissions). Also, interactions with other emissions, such as particulate matter, can contribute to emissions reductions. Approximately, 83 % of the NO_x emissions were reduced while around 90 % of the SO_2 and 73 % of the HCl were retained in the system (considering an average of the measured values). It is possible to verify that primary emission reduction measures assure that the legal ELVs are obeyed.

The O_2, CO, CO_2, NO_x and SO_2 concentrations along the sampling periods (measured through a CEMS from the PP) is presented in **Figure 24** and **Figure 25**.

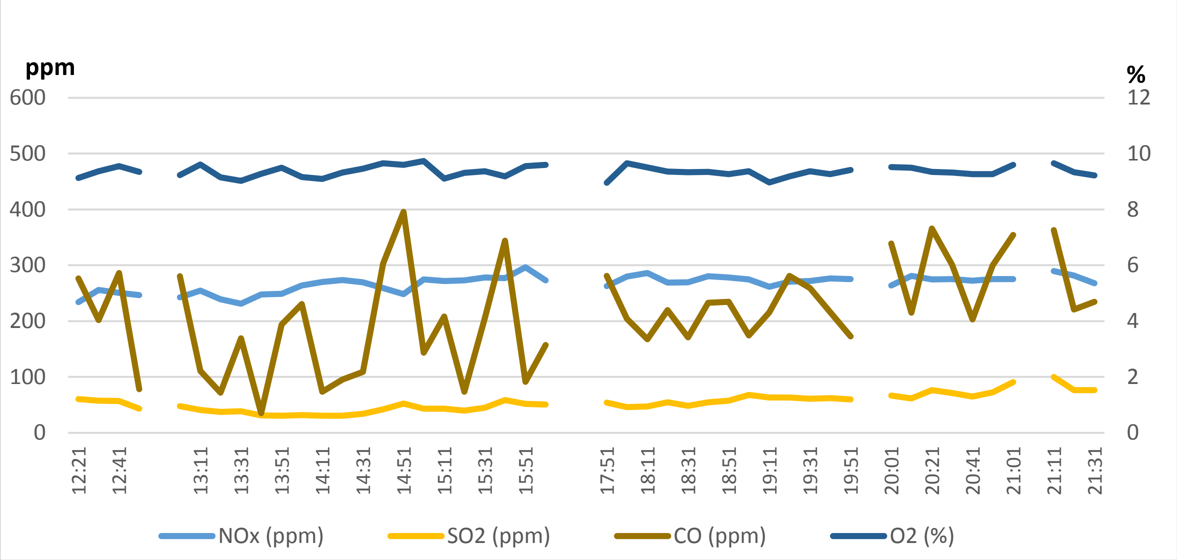

Figure 24 - *Day A: O_2, CO, NO_x and SO_2 emissions (CEMS data)*

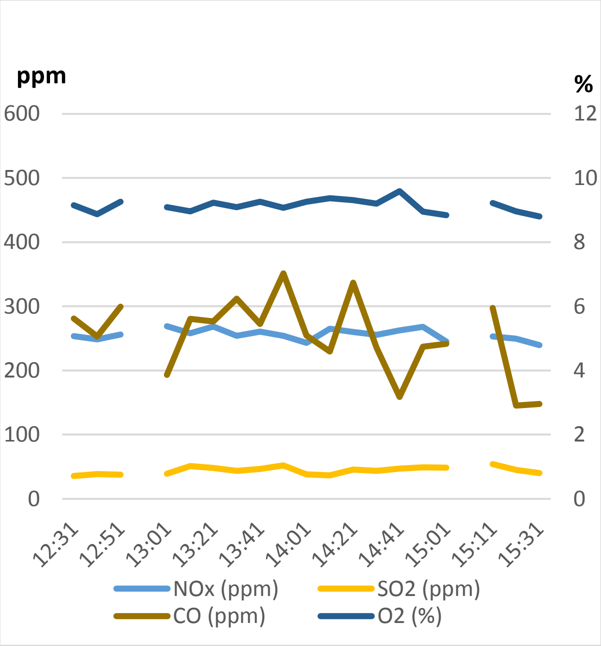

Figure 25 - *Day B: O_2, CO, NO_x and SO_2 emissions (CEMS data)*

It can mean that NO_x emissions were well controlled and the emissions were stabilized within a small range of variation. The range values are presented in Table 12.

Table 12 - *Flue gas O_2, CO, NO_x, and SO_2 ranges (CEMS data)*

Samplings	O_2 (%)	CO (mg/Nm³, 6%O₂)	NO_x	SO_2
TSPA and HClA1	9,0-9,7 (Δ=0,7)	45-510 (Δ=465)	298-382 (Δ=84)	39-76 (Δ=37)
TSPB and HClB	8,8-9,6 (Δ=0,8)	201-446 (Δ=245)	308-341 (Δ=33)	46-66 (Δ=20)
PMA	9,0-9,7 (Δ=0,7)	215-361 (Δ=146)	335-367 (Δ=32)	59-87 (Δ=28)
PGCA	9,3-9,6 (Δ=0,3)	263-473 (Δ=210)	341-363 (Δ=22)	80-117 (Δ=37)
HClA2	9,0-9,7 (Δ=0,7)	215-470 (Δ=255)	336-368 (Δ=32)	59-117 (Δ=58)

In the case of CO emissions the results ranged 465 ppm within the same sampling test; such was the case of the TSPA/HClA1 sampling with CO emissions between 45 ppm and 510 ppm. These emissions may be due to fluctuations in the biomass feeding system and/or may result from the heterogeneity of the biomass fed to the fluidised bed reactor.

Also SO_2 emissions presented fluctuations during the sampling period. However, these variations were not as significant as in the case of CO. Nevertheless, the range of SO_2 emissions may also reflect the heterogeneity of the biomass fuel since this pollutant is dependent on the fuel composition.

Solid biomass combustion behaviour, inside the boiler, is possible to observe through analysis of the CO emissions, since its emissions are an indicator of the combustion efficiency. This analysis is done using data from the TESTO analyser, with values collected every thirty seconds, which is more detailed than the data from CEMS, whose values are collected every ten minutes. Therefore, emission profile for O_2 (vol%), and CO (ppm) during the Day A are presented in **Figure 26 (A)**. TSPA, PMA and GA sampling periods are referenced to the O_2 and CO averages obtained during the respective period.

Fluctuation of O_2 and CO may be associated to the fact that when the biomass is fed into the boiler starts to devolatilise (this biomass has a high content of volatile matter: 72 % to 76 %), and due to the fast increase of fuel inside the boiler a peak of volatile gases is produced. Afterwards, CO gases mix with the surrounding air, with the help of the secondary air inlet, will be oxidized. Hence, the reaction with O_2 reduces the CO concentration in the combustion environment, leading to a decay on its profile. This behaviour is possible to observe, with detail in **Figure 26 (B)**.

It is possible to verify a variation on the CO emissions´ peaks, reaching a maximum of 5000 ppm while the daily average is 148 ppm. These peaks may be caused by the heterogeneous characteristics of this biomass, either chemically and granulometry. However, as can be seen in **Figure 26 (B)**, these peaks occur in very short periods of time, and the FB system quickly reacts and stabilize the CO and O_2 concentration to lower levels.

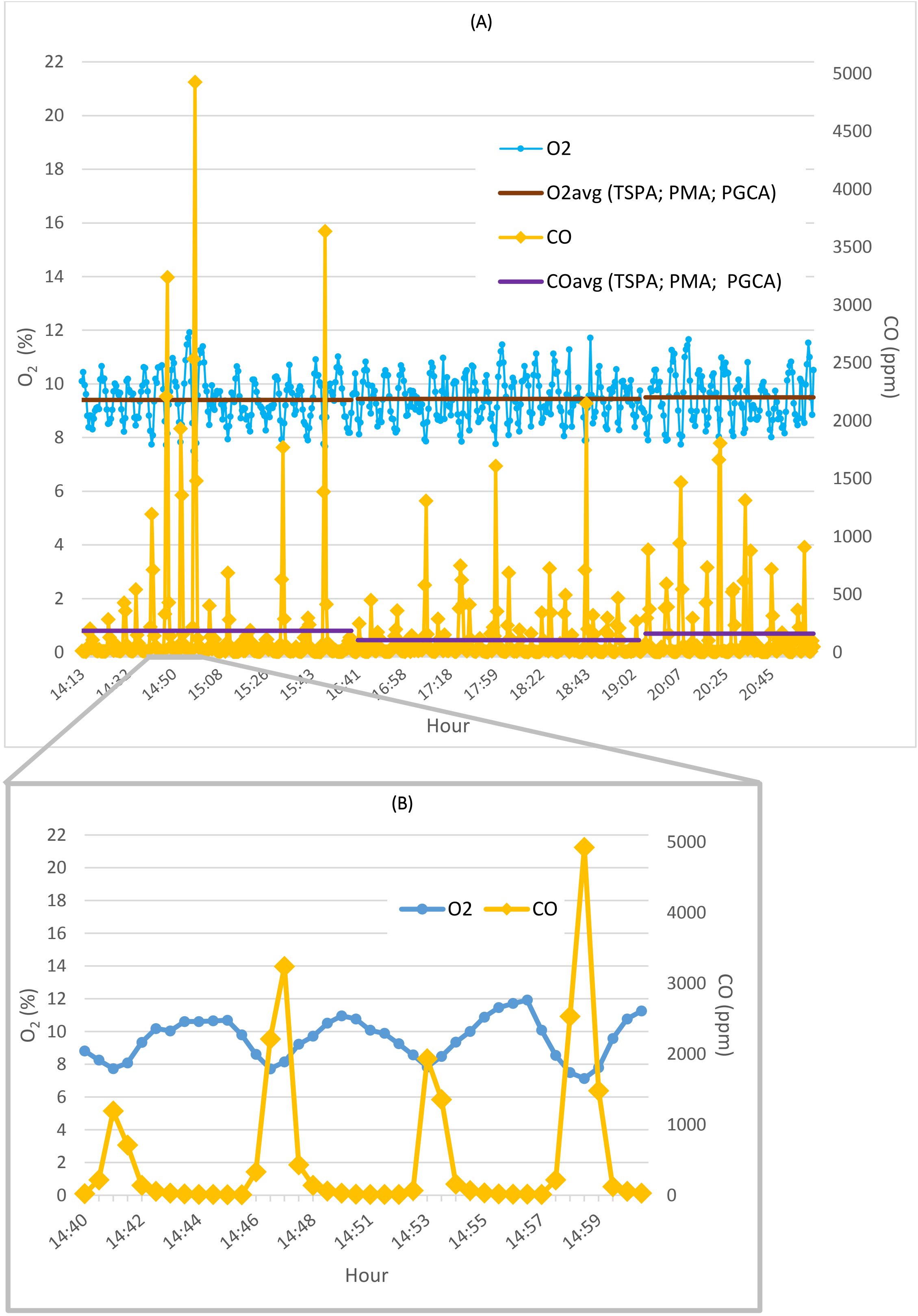

Figure 26 – ***(A)*** *O_2 and CO emissions profile for Day A;* ***(B)*** *O_2 and CO emissions profile for Day A - detail*

Post-sampling filters, with particles, were taken from the filter holder inside the hot box (TSP), from the Mark III (PGC) and from the TECORA MSSI ($PM_{10/2,5}$) and were weighted inside a petri box, as presented in **Figure 27**.

Figure 27 – *Filters with particles of sampling GA (Mark III), PMA(TECORA MSSI) and PTSB (TSP)*

All the particle collecting samplings are validated by the isokinetic rate obtained during sample, which comply with the ideal range defined by the methodologies.

3.2 TOTAL SUSPENDED PARTICLES

Total suspended particles were sampled according to the method mentioned in **Section 2.3.7,** during two different periods of 176 min and 120 min, respectively for TSPA and TSPB.

Concentration of TSP obtained for the two days may be considered very low. Normal sampling periods for this type of measurement take generally a maximum of one hour. However, from information obtained by the PP it was known that emissions were very low (< 5 mg/Nm^3, dry gas), thus sampling periods were longer (as mentioned before) in order to get measurable quantities of particles for calculation of this parameter.

Masses of particles, determined gravimetrically, were divided by the flue gas sample, corrected for PTN (Nm^3) and dry conditions (moisture of the flue gas measured in **Table 10**). Particles concentration, converted to the reference oxygen percentages (6 %, 8 % and 11 %), are shown in **Table 13**, for the two days.

Table 13 - TSP sampled concentration

	c_s (mg/Nm^3, dry gas)		
$\%O_{2,ref}$	6	8	11
TSPA	21,3	18,5	14,2
TSPB	(8,9)*	(7,7)*	(5,9)*

* underestimate due to filter damage

Although the ESP was partially shut down during TSPB, which could lead to higher concentration of emitted particles when compared to TSPA, the results do not comply with this prevision. This difference may be the result of the damaged filter after TSPB sampling, leading to a possible loss of filter's mass, augmented with a high uncertainty in the weighing procedure of low particle mass obtained. Also, given the low concentrations, difference in concentration may reflect fluctuation of emissions in different days.

However, the filters were suitable for further analysis, since the main purpose of this study was not to verify the emissions compliance with the ELV and due to time containments to perform another sample of this parameter.

3.2.1 TSP SEM/EDS ANALYSIS

Observations from the stereomicroscope and microprobe help to verify this assumption, by comparing figures from both sampling periods.

SEM analysis, shown in **Figure 28**, present the morphology of the collected particles, shown by scanning magnifications images of x1000 and x3500, as well their chemical composition given by spectrums. Analysed particles by EDS are here identified with a number, for easy understanding.

With observations at x3500 in the TSPA sample, it is possible to verify the predominance of small and individual particles over filter fibre, a probable result from nucleation or condensation of gaseous material, composed of Na and K (1). Detection of Al and Si, may be attributed to interference of filters made of glass fibre.

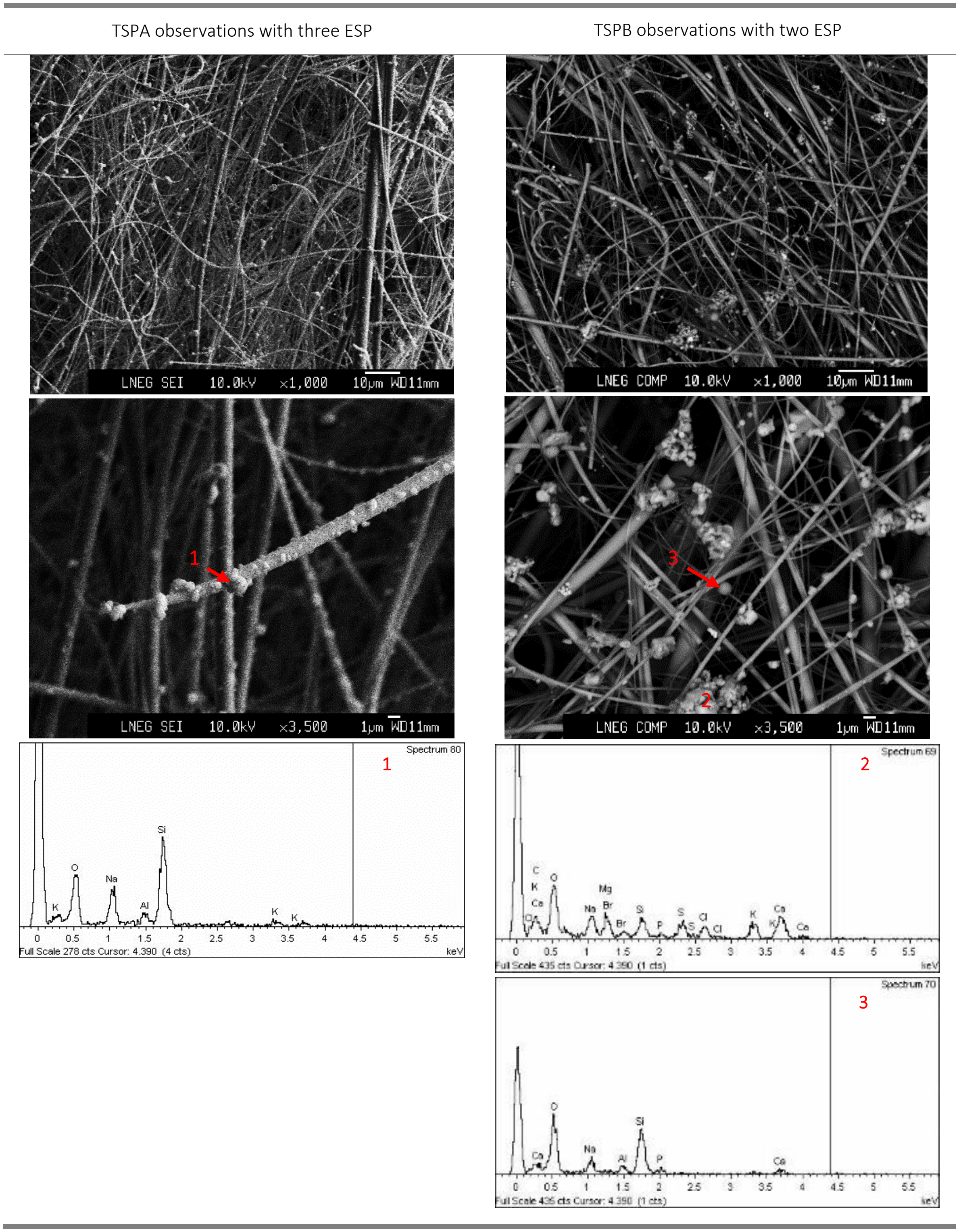

Figure 28 - *TSP samples SEM analysis*

The same observation – x3500 – in the TSPB sample, shows a higher variation of particles forms and chemical composition and morphology a possible effect of the ESP partial shut-down. Main observations are agglomerated particles (2) and cenospheres (3). Spectrum show that the particle agglomerates chemical composition contain various elements, due to different composition of various particles coagulated and possible heterogeneous condensation in the surface of other particles. While the cenosphere spectrum shows Al, Si and Na, which complies with the conclusion made for TSPA.

3.3 PARTICULATE CLASSIFICATION

The procedures for both Particulate Granulometric Classification and $PM_{10/2,5}$ sampling methods occurred as described in **Section 2.3.8** and **Section 2.3.9**, respectively.

PMA ($PM_{10/2,5}$ from day A) sample was obtained in a period where the ESP was partially shut-down. Due to lack of previous information on the amount of emitted particles, the recommended total sample period for this parameter was difficult to establish. Therefore, after the partial shut-down, half-way into the first hour of sampling, and due to low particle collection (detected by a small variation of pressure drop in the control unit), it was decided to extend this sample another full-hour. This fact resulted in an overload of the collected particles on the second stage (PMA_2), where the load should not exceed 3 mg.

During the PGCA (PGC from day A) the flue gas flow into the Mark III impactor varied when sampling was performed, causing an undesirably variation on the aerodynamic diameter of the collected particles. Adverse sampling conditions and flues gas flow's variation during sampling are identified as the main reasons to this situation.

These incidents led to consequences regarding the aerodynamic diameter distribution, leading to incoherent results on the mass collected by diameter class. Nevertheless, and as stated before, this study focus on the chemical and morphological constitution of the produced fly-ash particles of biomass combustion.

3.3.1 $PM_{10/2,5}$

The second plate of the TECORA MSSI, with a diameter range between 10 µm and 2,5 µm, presented a particle overload (105 mg against the recommended maximum of 3 mg per stage), due to a build-up of pyramid-like agglomerates of particles, over the collecting filters. This agglomerate was observed by an Olympus SZH stereo microscope with a coupled Olympus DP20 digital camera, as presented in **Figure 29**.

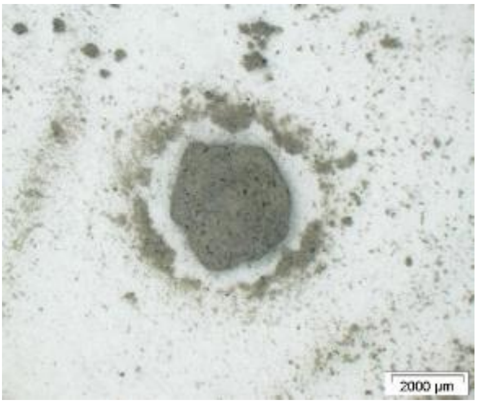

Figure 29 - Particle pyramid from PMA_2 sample

Twelve pyramids were formed, which correspond to the number of flow inlet holes on that plate. In the end these pyramids may have blocked the sample flow stream, by closing the cut-off stage inlets, preventing the flow, and the particles dragged with it, to impact in the backup filter (PMA_F). This resulted in higher concentration of PM_{10} particles, 47 mg/Nm^3, and less of $PM_{2,5}$, approximately 5 mg/Nm^3 (at 6%O_2 , dry gas).

Sample's SEM analysis is summarized in **Figure 30**. Since the second plate (PMA_2) and the backup filter (PMA_F) are most relevant for this parameter, the first plate (PMA_1) was not analysed by SEM.

SEM analysis show a high density of mixed particles, not allowing a specific particulate analysis. However, it was possible to observe the presence of chlorinated alkali compounds (2, 3, 4) and also cenosphere-like structures (1), in both the second and backup plate.

These observations required a better scattering of the sampled particles, in order to analyse the particles' chemical composition and morphology.

Filter	SEM Image	EDS Spectrum
PMA_2	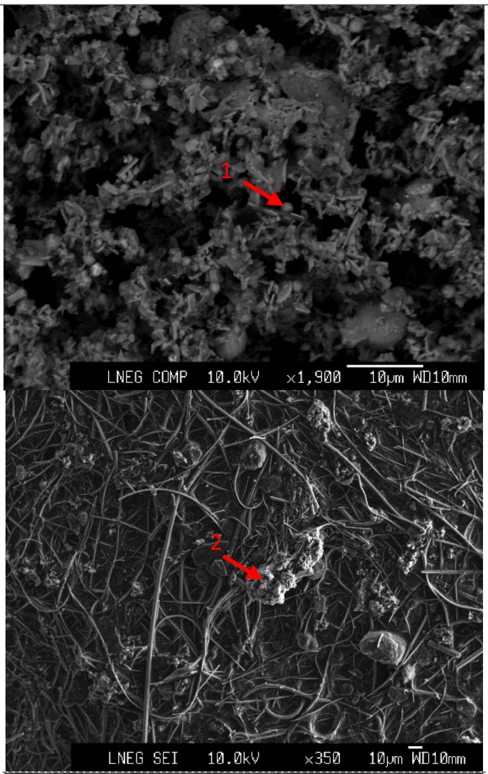	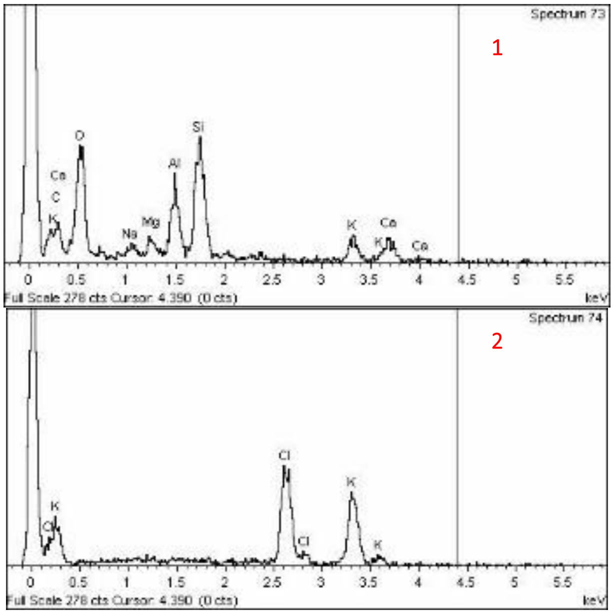
PMA_F	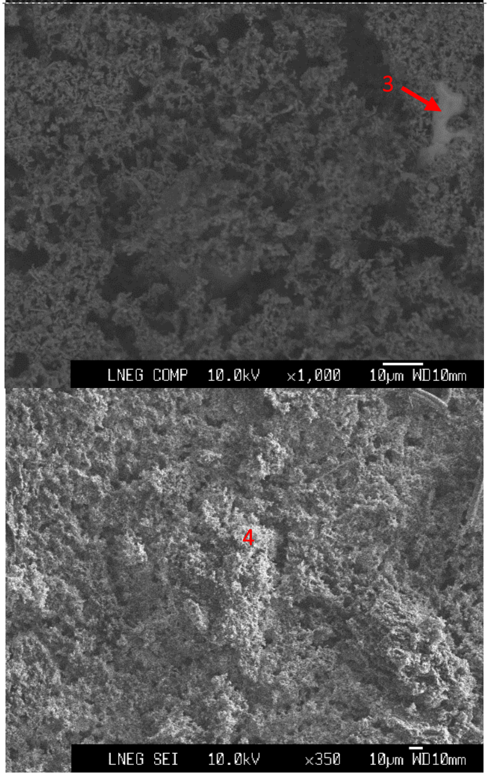	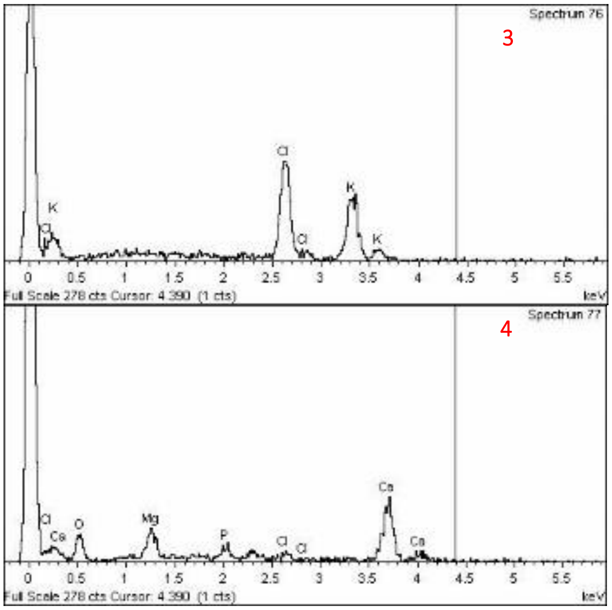

Figure 30 - *$PM_{10/2,5}$ sample SEM analysis*

3.3.2 PGC

The particle granulometric classification should be sampled at a constant flue gas flow, under isokinetic conditions, since the cut-off diameter depends on the flue gas flow, as explained in **Section 2.3.8**. Therefore, due to the adverse sampling conditions, which led to an undesirable variation on the flue gas flow sampling, the cut-off diameter for each stage was determined considering the average gas flow obtained during sampling.

Considering the *Mark III User Manual*'s chart of aerodynamic diameter as a function of the gas flow, the diameter values obtained were determined, for as average sampled gas flow of 1,9 acfm and stack temperature of 291 F (approx. 144 ^{o}C).**Figure 31** shows the cut-off diameters variation by stage: maximum, medium and minimum values correspond to gas flow's variation: 2,4 acfm, 1,9 acfm and 1,1 acfm, respectively.

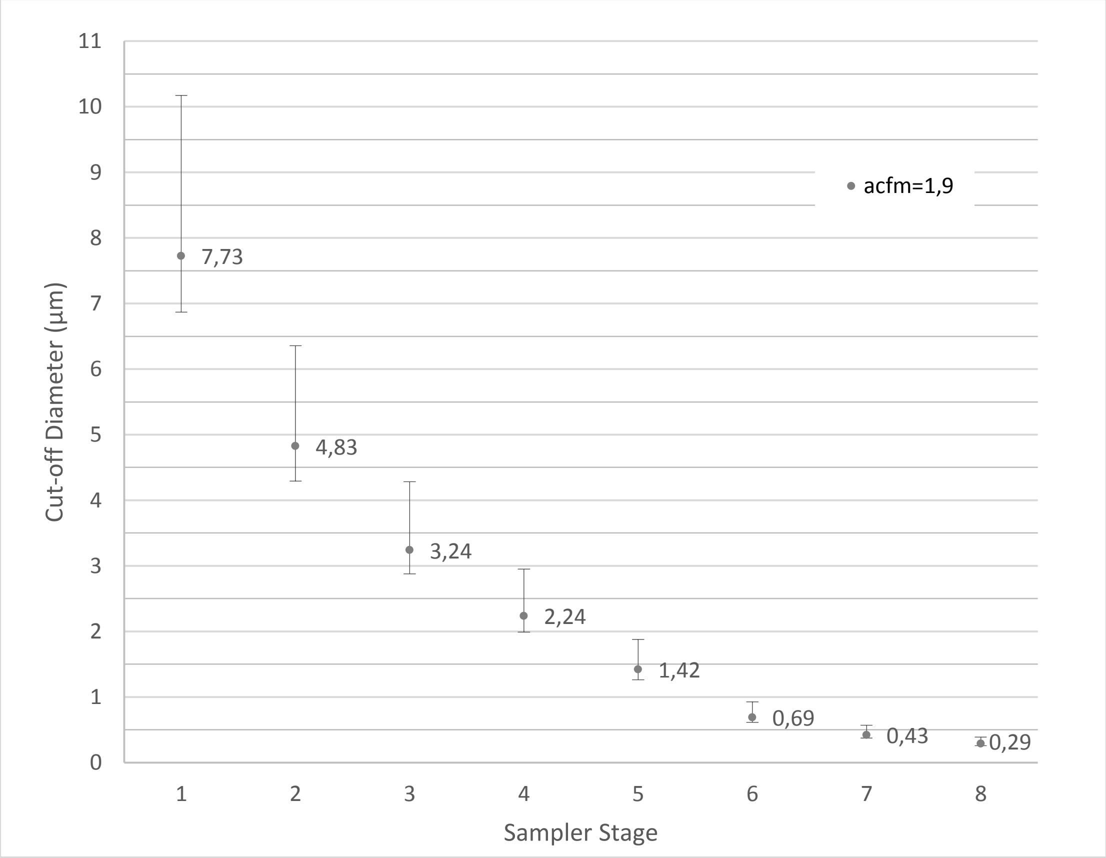

Figure 31 – *Cut-off diameter variation by stage (Mark III), due to sample flow variations*

The cut-off diameters determined are below 10 µm, in accordance with the application range of *Mark III*. This analysis shows the influence of the sampling flow on the aerodynamic diameter of the particle: to the maximum flow (2,4 acfm) corresponds the lower value of each diameters, while for the minimum flow (1,1 acfm) corresponds the higher value of each diameter.

It is important to notice how the diameter ranges of each impactor stage do not overlap from stage to stage. There are two situations where the lower value of the upper stage is equal to the higher value of the lower stage: stage 2 to stage 3 and stage 3 to stage 4. The diameter range of each stage decreases with stage number, bigger diameters have a higher variation on the diameter's range.

Therefore, by this analysis, three stages were in the submicron (<1 µm) range of aerodynamic diameters: PGCA_7/8/F.

With a total collected particles mass of 30,9 mg, the percentage distribution and cumulative percentage by aerodynamic diameter is shown in **Figure 32.**

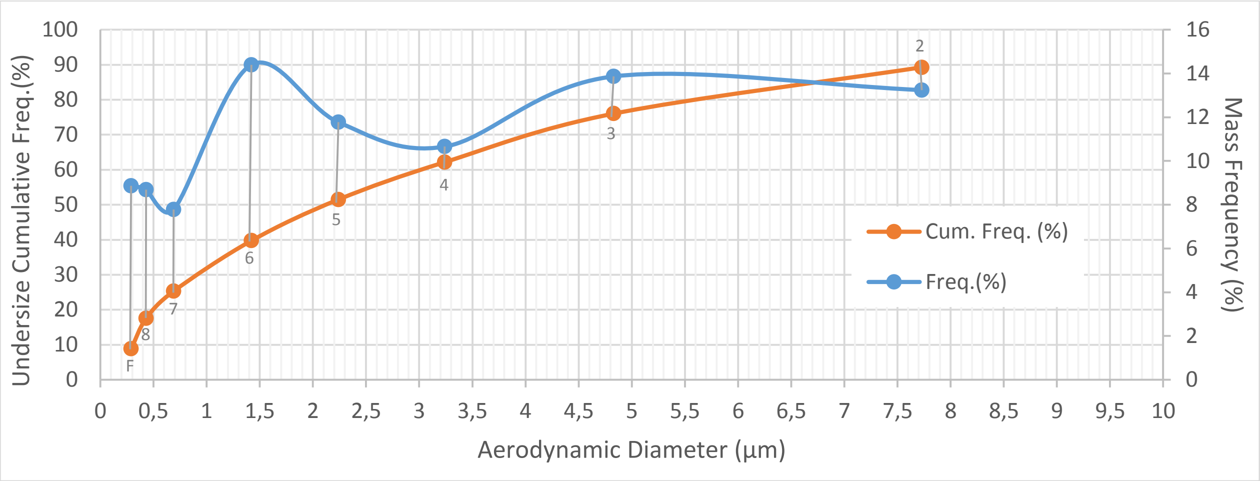

Figure 32 – PGC sample mass frequency and cumulative frequency, by impactor stage

The distribution of particles by diameter is also influenced by the same adverse conditions which affected the cut-off diameter variation. The frequency distribution shows three modes corresponding to: the backup filter (0,29 µm); PGC_6 (1,42 µm); PGC_3 (4,83 µm).

From the cumulative frequency analysis it is determined that 50 % of the collected particles mass have an aerodynamic diameter below 2,13 µm, below stage 4 of the impactor. Therefore, the SEM observations for the PGC samples was focused on the smaller diameter ranges (stage 5 to backup filter).

Table 14 summarizes the aerodynamic diameter (µm) and the particles concentrations converted to reference oxygen percentages, corrected for PTN (Nm^3) and dry conditions.

Table 14 - PGC aerodynamic diameters and concentrations for each impactor stage

Stage	Aerodynamic diameter (µm)	c_s (mg/Nm^3, dry gas)		
		6 %O_2	8 %O_2	11 %O_2
1	>7,73	3,0	2,4	1,9
2	7,73	3,5	3,0	2,3
3	4,83	3,6	3,1	2,4
4	3,24	2,8	2,4	1,9
5	2,24	3,1	2,7	2,1
6	1,42	3,8	3,3	3,0
7	0,69	2,0	1,8	1,4
8	0,43	2,3	2,0	1,5
F	0,29	2,3	2,0	1,5

Relevant SEM observations with the corresponding EDS spectrums, are summarized in **Figure 33.**

Overall, alkali compounds were detected in all of the analysed stages. Calcium was detected in most of the observations (1, 3, 5, 7, 8, 10, 11), expectable fact due to the biomass high content of this element. From the observation of particle 7, the spectrum detected higher quantity of Ca than other element, followed by Cl. Due to the high affinity of reaction between these elements, the particle is probably $CaCl_2$. This salt is solid at ambient temperature. In the observation presents molten-like morphology. Particle (1), $CaSO_4$ from EDS observation, is a crystal of calcium sulphate. In this same particle also small quantities of Cl were detected. These particles may be a result of chlorination and sulphation of the elements, *i.e.* the chemical reaction of elements with chlorine (Cl) and sulphur (S).

These results are consistent with the conclusions presented by Laursen *et al.* (2002) and Partanen *et al.* (2005a) that found sulphur retentions for $n_{Ca}/n_S > 3$ and chlorine retentions for $n_{Ca}/n_{Cl} > 2$, in this fuel the molar ratios were $n_{Ca}/n_S = 6,3$ and $n_{Ca}/n_{Cl} = 7,6$.

Fuel-bound sodium also reacts with Cl and S, from fuel and bed material from the boiler, produce compounds such as NaCl (9), Na_2SO_4. This particle presents a molten crystal morphology. Next to this compound of non-volatile ash elements (8) is observed.

Potassium evapourates with chlorine to originate KCl (2, 6, 13), these particles present crystal shape and are present in every range of diameters.

The high observation of chlorine complies with the significant amount of HCl collected during PGCA sampling, around 40,5 mg/Nm^3 (10%O_2, d.b.), more detailed explanation in **Section 1.3.4**. Chlorine is highly responsible for alkali volatilisation.

Silica (SiO_2) enters the system in fuel's constitution, 0,6 % to 2,44 %, bed material (sand) and a probable fuel contamination (rocks and soil). Si originates vitrinite like structures similar to cenosphere (3), as found in TSPB as well, and it is present in many stages of the impactor together with other elements (5, 7, 8, 11), the last three particles resemble melted structures.

The presence of Fe (4) and Mg is spotted in particle agglomerates (5) and melted compounds with Si and P alkali metals and other. These elements appear as Fe_2O_3 and MgO from the fuel composition.

Barium is detected in (12) although it was not considered for the fuel's characterization. This alkaline earth metal, may have a clear origin in the fuel's contamination, or from its heterogeneous composition and origin.

Lead (Pb), which raises health concerns regarding the nervous system, was detected in a submicron range of aerodynamic diameters (< 0,43 µm). It is identified by the glowing spots in a fusion produced mixture of non-volatile and alkali elements. This element, an heavy metal, either is volatilized as chloride, $PbCl_2$, or goes under heterogeneous condensation on other particles surfaces, as shown in **Figure 3**, with K_2SO_4 and KCl, elements detected in (10, 11). Also, Pb is reactive with aluminosilicates (Nussbaumer, 2001), which are also found in the mixture.

Although, this element has relatively low share in the fuel's composition – 2 mg/kg to 6 mg/kg – the fact that it is emitted with the submicron diameter range of particles, and it is detected in the EDS analyses, shows that this element easily volatilises with other elements.

<table>
<tr><th>Filter</th><th>Aerodynamic Diameter (µm)</th><th>SEM Image</th><th>EDS Spectrum</th></tr>
<tr><td>GA_1</td><td>>7,73</td><td>
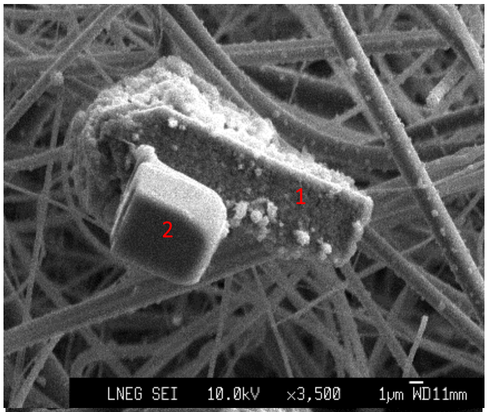

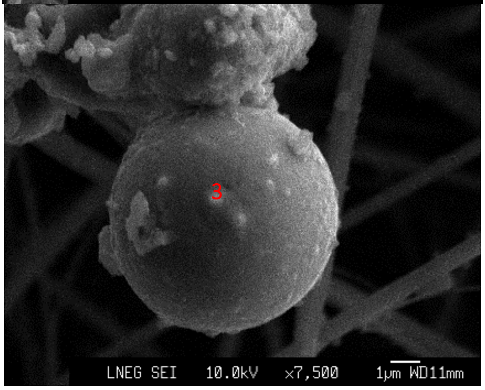

</td><td>
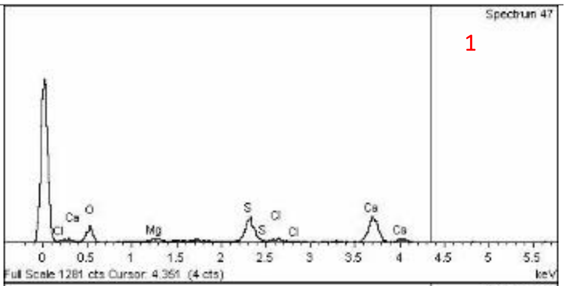

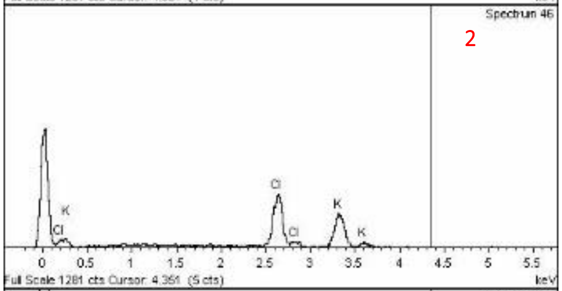

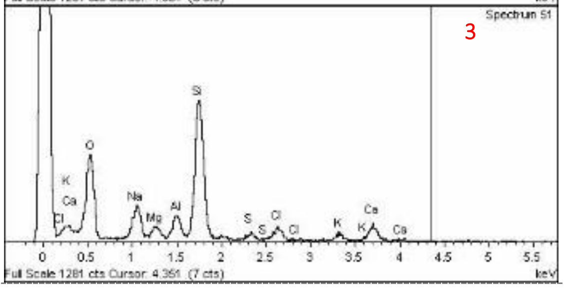

</td></tr>
<tr><td>GA_5</td><td>2,24</td><td>
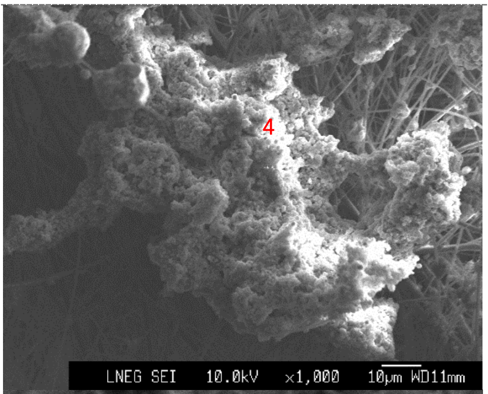

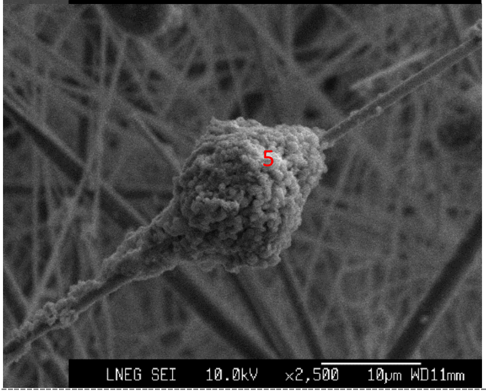

</td><td>
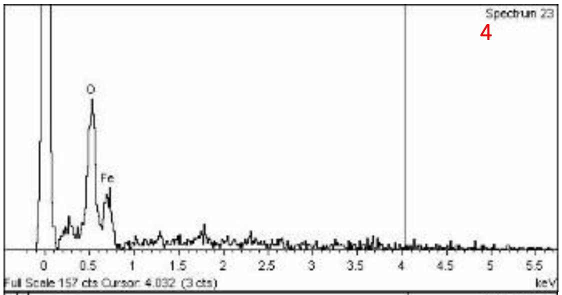

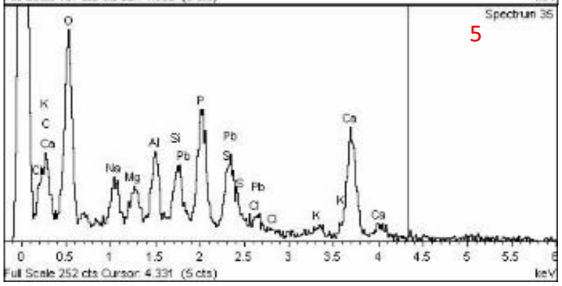

</td></tr>
</table>

<table>
<tr><th>Filter</th><th>Aerodynamic Diameter (µm)</th><th>SEM Image</th><th>EDS Spectrum</th></tr>
<tr><td>GA_6</td><td>1,42</td><td>
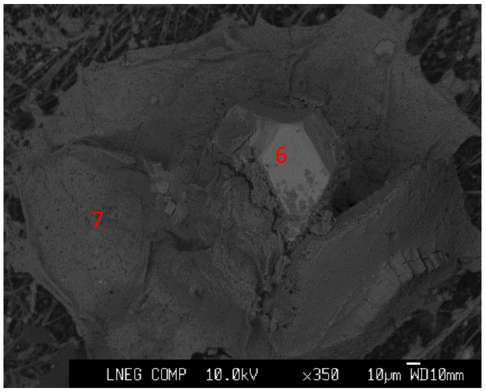

</td><td>
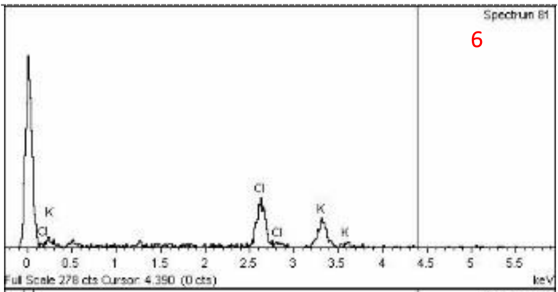

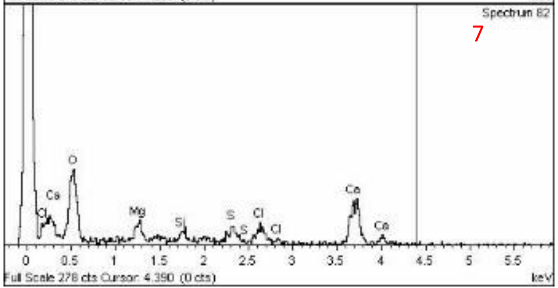

</td></tr>
<tr><td>GA_7</td><td>0,69</td><td>
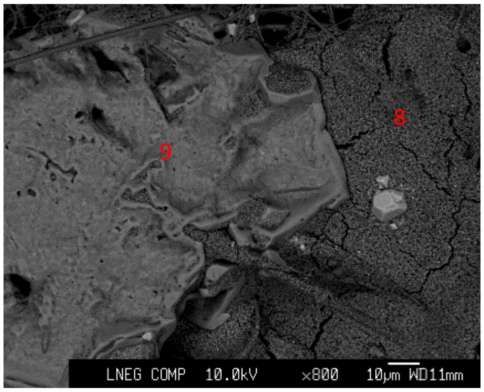

</td><td>
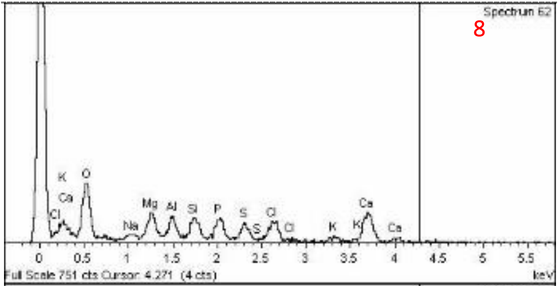

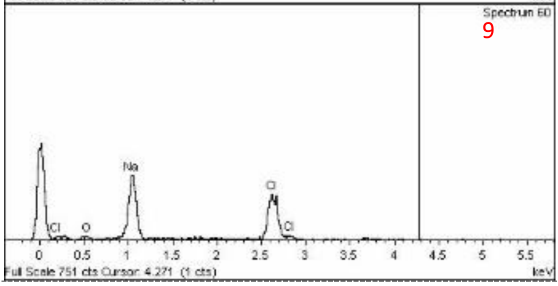

</td></tr>
</table>

Filter	Aerodynamic Diameter (µm)	SEM Image	EDS Spectrum
GA_8	0,43	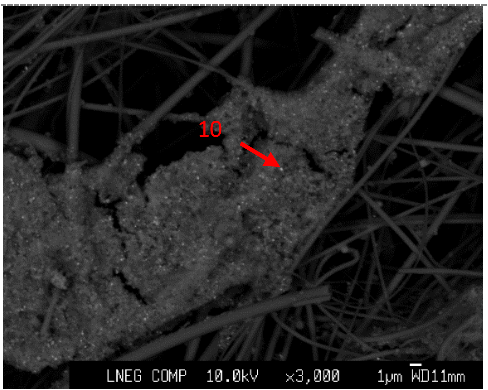 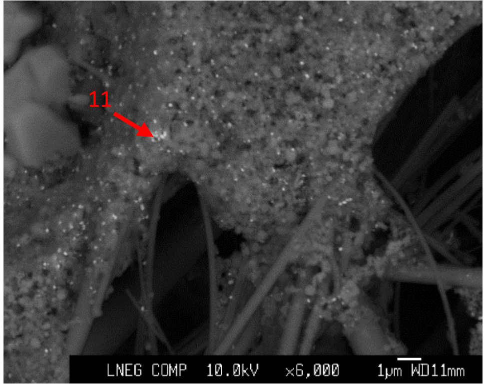	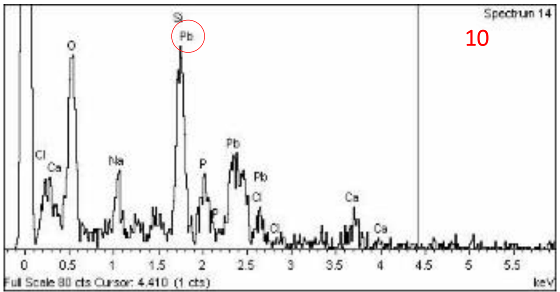 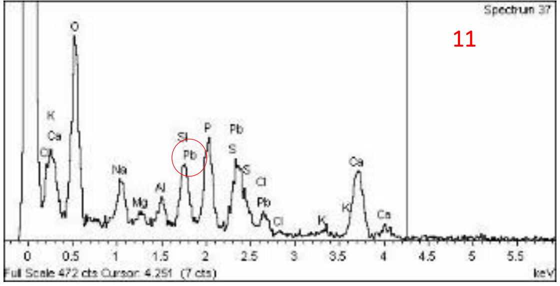
GA_FF	0,29	 	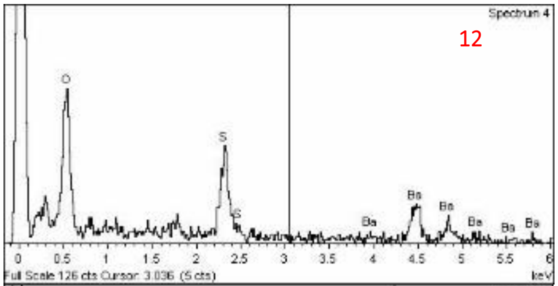 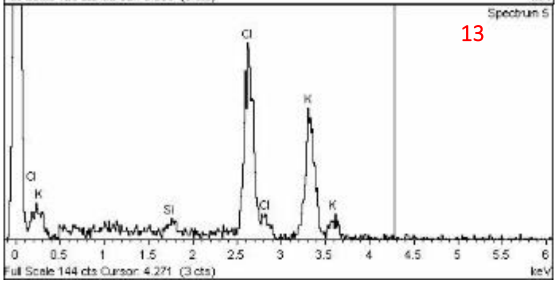

Figure 33 - *PGC samples SEM analysis*

4 CONCLUSIONS

The *in situ* sampling at industrial units revealed to be a complex and highly demanding process. The biggest restraint was the lack of time to perform more samples for each parameter, also the amount and type of materials/equipment used in the sampling.

The biomass-fired FB combustion system retains most of its pollutant emissions (measured by a CEMS from the PP) of SO_2, NO_x and HCl (collected according to an internal method based in EN 1911), with retentions around, 90 %, 83 % and 73 %, respectively. These retentions were related not only with the biomass high alkali content (such as calcium) and controlled combustion using primary emission reduction measures, without the need of major flue gas cleaning equipment.

SO_2, NO_x found obey ELV levels, but HCl emissions are not controlled for the biomass-fired combustion systems. However, due relevant concentrations of HCl collected (28,2 mg/Nm^3, 31,4 mg/Nm^3 and 40,5 mg/Nm^3 at 10 % O_2), and denoting the ELV from the IED (2010) for waste co-incineration systems (10 mg/Nm^3 at 10 % O_2), it is possible to understand the urge for legislation to control HCl emissions for biomass-fired systems.

Particulate matter was sampled following the method for Total Suspended Particles (TSP) and, in order to study the particulate size distribution and morphology of particles in function to their diameter, the $PM_{10/2,5}$ and Particulate Granulometric Classification methods were used.

The ELV for the particulate matter (30 mg/Nm^3 at 6 % O_2), from the medium combustion plants directive proposal (MCP, 2013), is considered for the PM emissions analysis. Hence, none of the samples collected surpassed that limit, the higher amount collected was 21,3 mg/Nm^3 (6 % O_2) during the TSP sampling in one of the sampling periods (Day A). The PP has a highly efficient particle removal

ESP which assures that the ELV for PM (dust) is complied. Even with the ESP working at approximately 66 % of its capacity during the sampling periods (TSPB, $PM_{10/2,5}$, and PGC) the emissions values still low and under legal limits.

However, the purpose of this work is to study the chemical and morphological constitution of the produced fly-ash particles of biomass combustion, and understand its presence in different particle's aerodynamic diameter, not to evaluate compliance with different regulations, which may change with time.

For an aerodynamic diameter range below 10 µm (using eight stage *Mark III*, PGC method) the presence of alkali compounds in the collected particles was detected regardless of the stage, as well as chlorine. This shows the influence of the fuel's constitution on its combustion emissions, as Cl were very significant.

The presence of Lead (Pb), a heavy metal (HM) which raises environmental and health concerns, was detected in a submicron range of aerodynamic diameters (< 0,43 µm), even though the fuel had a relatively low share of this element in its composition. The fly-ash control of biomass-fired PP must focus on the small diameter particles (finer, aerosols), since these particles may contain higher concentration of HM, due to their high volatile tendencies, together with the alkali metals. This concern increases once these finer particles have higher probability to be inhale and enter the blood stream of an exposed individual, causing health problems.

Another detected element in the SEM analysis was silica (Si), which may have origin in the fuel, fluidized bed material (silica) and also from the sampling filter's fibres (glass fibre). Also, another origin is the fuel contamination, of soil/sand and rocks, which could be reduced by a fuel pre-treatment to remove these contaminators.

It is important to state that these results are for study and training purposes only and, therefore, are representative of the installation emission values.

As future work, more samples for each parameter should be performed, in particular for the $PM_{10/2,5}$ and PGC, in order to study the finer particles behaviour and composition. As well the SEM analysis should be conducted more intensely since its results are highly important, although preparation for observation has to be improved given the difficulties to observe very small particles in glass fibre filters.

5 REFERENCES

. Alakangas, E., Junginger, M., van Dam, J., Hinge, J., Keränen, J., Olsson, O., . . . Vinterbäck, J. (2012). EUBIONET III—Solutions to biomass trade and market barriers. *Renewable and Sustainable Energy Reviews, 16*(6), 4277-4290. doi: http://dx.doi.org/10.1016/j.rser.2012.03.051

Babcock, B. W. C. (2005). Steam : its generation and use with catalogue of the manufactures of the Babcock and Wilcox Company (pp. v.). New York: The Company.

BAT. (2006). Reference Document on Best Available Techniques for Large Combustion Plants. *Integrated Pollution Prevention and Control*.

Bayless, D. J., Alam, M. K., Radcliff, R., & Caine, J. (2004). Membrane-based wet electrostatic precipitation. *Fuel Processing Technology, 85*(6–7), 781-798. doi: http://dx.doi.org/10.1016/j.fuproc.2003.11.025

BREF. (2006). Reference Document on Best Available Techniques for Large Combustion Plants.

Castle, G. S. P. (2001). Industrial applications of electrostatics:: the past, present and future. *Journal of Electrostatics, 51–52*(0), 1-7. doi: http://dx.doi.org/10.1016/S0304-3886(01)00068-7

CAFE. (2008). Directive 2008/50/EC on Ambient Air Quality and cleaner air for Europe

Chang, R. (1992). Compact hybrid particulate collector (COHPAC): Google Patents.

Cherubini, F., Peters, G. P., Berntsen, T., StrØMman, A. H., & Hertwich, E. (2011). CO2 emissions from biomass combustion for bioenergy: atmospheric decay and contribution to global warming. *GCB Bioenergy, 3*(5), 413-426. doi: 10.1111/j.1757-1707.2011.01102.x

DGEG. (2014). Renováveis - Direcção Geral de Energia e Geologia *Estatísticas Rápidas - nº 111 - maio de 2014*.

Duarte Fo, O. B., Marra, W. D., Kachan, G. C., & Coury, J. R. (2000). Filtration of Electrified Solid Particles. *Industrial & Engineering Chemistry Research, 39*(10), 3884-3895. doi: 10.1021/ie0002430

EC, E. C. (2005). Biomass action plan COM(2005) 628 final.

EC, E. C. (2011, 10/04/2015). Towards a competitive low-carbon energy sector. Retrieved 12/04/2015, from http://ec.europa.eu/news/energy/111219_en.htm

EC, E. C. (2015, 26/03/2015). The 2020 climate and energy package. Retrieved 12/04/2015, from http://ec.europa.eu/clima/policies/package/index_en.htm

EN1911. (2010). Stationary source emissions - Determination of mass concentration of gaseous chlorides expressed as HCl – Standard reference method.

EN14790. (2005). Stationary source emissions - Determination of the water vapour in ducts: European Committee for Standardization.

EPA1. Method 1 - Sample and Velocity Traverses for Stationary Sources.

EPA2. Method 2 - Determination of Stack Gas Velocity and Volumetric Flow Rate (Type S Pitot Tube).

EPA3. Method 3 - Gas Analysis for the Determination of Dry Molecular Weight.

EPA3A. Determination of oxygen and carbon dioxide concentrations in emissions from stationary sources (instrumental analyzer procedure).

EPA5. Method 5 - Determiantion of particulate matter emissions from stationary sources.

EPA6C. Determination of sulfur dioxide emissions from stationary sources (instrumental analyzer procedure).

EPA7E. Determination of nitrogen oxides emissions from stationary sources (instrumental analyzer procedure).

EPA10. Determination of carbon monoxide emissions from stationary sources (instrumental analyzer procedure).

EPA26A. Method 26A - Determination of hydrogen halide and halogen emissions from stationary sources isokinetic method.

EPA. (2013, 11/06/2013). PM2.5 NAAQS Implementation. Retrieved 22/10/2014, 2014, from http://www.epa.gov/ttn/naaqs/pm/pm25_index.html

EurObserv'ER. (2013). Solid Biomass Barometer.

Fuertes, A. B., Artos, V., Pis, J., Marbán, G., & Palacios, J. (1992). Sulphur retention by ash during fluidized bed combustion of bituminous coals. *Fuel, 71*(5), 507-511. doi: http://dx.doi.org/10.1016/0016-2361(92)90147-G

Gulyurtlu, I. A., P. ; Boavida, D. ; Lopes, H. ; Cabrita, I. (2004). Considerations for Mixing Different Biomass Fuels and Non-Toxic Waste During Fluidised Bed Combustion *World biomass conference; biomass for energy industry and climate protection* (pp. 4). WIP-Munich, , Florence:.

Henriques, M. (2013). Effect of Exhaust Gas Recirculation and Air Staging on Gaseous and Particle Emissions in a Domestic Boiler (M. E. Departmentfenix, Trans.). In M. Costa (Ed.). Mechanical Engineering Department: Instituto Superior Técnico, Technical University of Lisbon, Lisbon, Portugal.

IED. (2010). DIRECTIVE 2010/75/EU on Industrial Emissions (integrated pollution prevention and control).

INEGI. e2p - endogenous energies of Portugal. Retrieved 08, 2014, from http://e2p.inegi.up.pt/

ISO14961. (2005). Solid biofuels - Fuel specifications and classes. Brussels: European Committee for Standardization.

Jaworek, A., Krupa, A., & Czech, T. (2007). Modern electrostatic devices and methods for exhaust gas cleaning: A brief review. *Journal of Electrostatics, 65*(3), 133-155. doi: http://dx.doi.org/10.1016/j.elstat.2006.07.012

Jenkins, B. M., Baxter, L. L., Miles Jr, T. R., & Miles, T. R. (1998). Combustion properties of biomass. *Fuel Processing Technology, 54*(1–3), 17-46. doi: http://dx.doi.org/10.1016/S0378-3820(97)00059-3

Khan, A. A., Aho, M., de Jong, W., Vainikka, P., Jansens, P. J., & Spliethoff, H. (2008). Scale-up study on combustibility and emission formation with two biomass fuels (B quality wood and pepper plant residue) under BFB conditions. *Biomass and Bioenergy, 32*(12), 1311-1321. doi: http://dx.doi.org/10.1016/j.biombioe.2008.03.011

Khan, A. A., de Jong, W., Jansens, P. J., & Spliethoff, H. (2009). Biomass combustion in fluidized bed boilers: Potential problems and remedies. *Fuel Processing Technology, 90*(1), 21-50. doi: DOI 10.1016/j.fuproc.2008.07.012

Krigmont, H., & Akishev, Y. (2008). Multi-stage collector for multi-pollutant control: Google Patents.

Laursen, K., & Grace, J. R. (2002). Some implications of co-combustion of biomass and coal in a fluidized bed boiler. *Fuel Processing Technology, 76*(2), 77-89. doi: http://dx.doi.org/10.1016/S0378-3820(02)00021-8

Lee, B.-K., Jung, K.-R., & Park, S.-H. (2008). Development and application of a novel swirl cyclone scrubber—(1) Experimental. *Journal of Aerosol Science, 39*(12), 1079-1088. doi: http://dx.doi.org/10.1016/j.jaerosci.2008.07.010

Lin, W. G., Dam-Johansen, K., & Frandsen, F. (2003). Agglomeration in bio-fuel fired fluidized bed combustors. *Chemical Engineering Journal, 96*(1-3), 171-185. doi: DOI 10.1016/j/cej.2003.08.008

Lind, T., Hokkinen, J., Jokiniemi, J. K., Saarikoski, S., & Hillamo, R. (2003). Electrostatic Precipitator Collection Efficiency and Trace Element Emissions from Co-Combustion of Biomass and Recovered Fuel in Fluidized-Bed Combustion. *Environmental Science & Technology, 37*(12), 2842-2846. doi: 10.1021/es026314z

Londahl, J., Pagels, J., Boman, C., Swietlicki, E., Massling, A., Rissler, J., . . . Sandstrom, T. (2008). Deposition of biomass combustion aerosol particles in the human respiratory tract. *Inhalation Toxicology, 20*(10), 923-933. doi: Doi 10.1080/08958370802087124

Lopes, H. (2013). Bias-to-Soil - Cinzas de biomassa: Características em relação à sua origem, tratamento e aplicação no solo - Relatório Intenro.

Lopes, H., Gulyurtlu, I., Abelha, P., Crujeira, T., Salema, D., Freire, M., . . . Cabrita, I. (2009). Particulate and PCDD/F emissions from coal co-firing with solid biofuels in a bubbling fluidised bed reactor. *Fuel, 88*(12), 2373-2384. doi: DOI 10.1016/j.fuel.2009.02.024

LRTAP. (2014). 1998 Protocol on Heavy Metals, as amended on 13 December 2012. *Executive Body for the Convention on Long-range Transboundary Air Pollution*.

Marques, F. (2013). Relatório Comissão de Agricultura e Mar - Grupo de Trabalho da Biomassa. Lisboa.

MCP. (2013). Proposal for a Directive on the limitation of emissions of certain pollutants into the air from medium combustion plants.

Miller, S. J. (2003). Advanced hybrid particulate collector and method of operation: Google Patents.

Naylor, T. B. (2009). *Flue gases : research, technology and economics*. New York: Nova Science Publishers.

Nifuku, M., Zhou, Y., Kisiel, A., Kobayashi, T., & Katoh, H. (2001). Charging characteristics for electret filter materials. *Journal of Electrostatics, 51–52*(0), 200-205. doi: http://dx.doi.org/10.1016/S0304-3886(01)00117-6

NPEN13284-1. (2009). Stationary source emissions - Determination of low range mass concentration of dust - Part 1: Manual gravimetric method: European Committee for Standardization.

NPISO10780. (2000). Stationary source emissions -- Measurement of velocity and volume flowrate of gas streams in ducts: European Committee for Standardization.

NPISO23210. (2009). Stationary source emissions - Determination of PM10/PM2,5 mass concentration in flue gas - Measurement at low concentrations by use of impactors: European Committee for Standardization.

Nussbaumer, T. (2001). *Aerosols from biomass combustion*: Verenum.

Nussbaumer, T. (2003). Combustion and co-combustion of biomass: fundamentals, technologies, and primary measures for emission reduction. *Energy & Fuels, 17*(6), 1510-1521. doi: Doi 10.1021/Ef030031q

Obernberger, I. (2005). *Ash related problems in biomass combustion plants*. Technische Universiteit Eindhoven.

Obernberger, I., Biedermann, F., Widmann, W., & Riedl, R. (1997). Concentrations of inorganic elements in biomass fuels and recovery in the different ash fractions. *Biomass and Bioenergy, 12*(3), 211-224. doi: http://dx.doi.org/10.1016/S0961-9534(96)00051-7

Obernberger, I., Brunner, T., & Bärnthaler, G. (2006). Chemical properties of solid biofuels—significance and impact. *Biomass and Bioenergy, 30*(11), 973-982. doi: http://dx.doi.org/10.1016/j.biombioe.2006.06.011

OECD. (1991). Estimation of greenhouse gas emissions and sinks. Paris.

Partanen, J., Backman, P., Backman, R., & Hupa, M. (2005a). Absorption of HCl by limestone in hot flue gases. Part II: importance of calcium hydroxychloride. *Fuel, 84*(12–13), 1674-1684. doi: 10.1016/j.fuel.2005.02.012

Partanen, J., Backman, P., Backman, R., & Hupa, M. (2005b). Absorption of HCl by limestone in hot flue gases. Part III: simultaneous absorption with SO2. *Fuel, 84*(12–13), 1685-1694. doi: http://dx.doi.org/10.1016/j.fuel.2005.02.013

PNAER. (2009). PLANO NACIONAL DE ACÇÃO PARA AS ENERGIAS RENOVÁVEIS AO ABRIGO DA DIRECTIVA 2009/28/CE.

Salcedo, R. L. R., Chibante, V. G., Fonseca, A. M., & Cândido, G. (2007). Fine particle capture in biomass boilers with recirculating gas cyclones: Theory and practice. *Powder Technology, 172*(2), 89-98. doi: http://dx.doi.org/10.1016/j.powtec.2006.10.027

Salema, D. (2008). *Co-Combustão de Biomassa e Carvão em Leito Fluidizado: Impactes nas emissões atmosféricas de NOx, SO2, CO, Dioxinas e Furanos e Material Particulado.* (Mestre em Bioenergia), Universidade Nova de Lisboa. Faculdade de Ciências e Tecnologia.

Schmidt, M., & Löffler, F. (1992). Investigations on fine particle separation using an electrostatic nozzle scrubber. *Journal of Aerosol Science, 23, Supplement 1*(0), 773-777. doi: http://dx.doi.org/10.1016/0021-8502(92)90526-2

Singh, R., & Shukla, A. (2014). A review on methods of flue gas cleaning from combustion of biomass. *Renewable and Sustainable Energy Reviews, 29*(0), 854-864. doi: http://dx.doi.org/10.1016/j.rser.2013.09.005

Sloss, L. L., & Smith, I. M. (2000). PM10 and PM2.5: an international perspective. *Fuel Processing Technology, 65*, 127-141. doi: Doi 10.1016/S0378-3820(99)00081-8

Tarelho, L. A. C., Coelho, A. M. S. L., Teixeira, E. R., Rajamma, R., & Ferreira, V. M. (2011). Characteristics of ashes from two Portuguese biomass co-generation plants. *19th European Biomass Conference and Exhibition*. Berlin, Germany.

Tarelho, L. A. C., Lopes, M. H. S. D., Silva, D. F. R. F., M.S.M., Teixeira, E. R., & Modolo, R. C. E. (2014). *Characteristics of biomass used as fuel and ashes produced in two thermal power plants with BFBC.* Paper presented at the World Bioenergy 2014., Elmia, Jönköping, Sweden.

Tarelho, L. A. C., Matos, M. A. A., & Pereira, F. J. M. A. (2005). The influence of operational parameters on SO2 removal by limestone during fluidised bed coal combustion. *Fuel Processing Technology, 86*(12-13), 1385-1401. doi: DOI 10.1016/j.furpoc.2005.03.002

Tarelho, L. A. C., Teixeira, E. R., Silva, D. F. R., Modolo, R. C. E., Silva, A. P. D., Gomes, C., . . . Freire, M. S. M. (2013, 3-7 June 2013). *Forest biomass residues combustion in a thermal power plant with FBC and ash characteristics and management options.* Paper presented at the 21st European Biomass Conference and Exhibition, Copenhagen, Denmark.

TECORA. (2015). MSSI. Retrieved 26/01/2015, 2015, from http://www.tecora.com/en/emission/1176-mssi.html

Torvela, T., Tissari, J., Sippula, O., Kaivosoja, T., Leskinen, J., Virén, A., . . . Jokiniemi, J. (2014). Effect of wood combustion conditions on the morphology of freshly emitted fine particles. *Atmospheric Environment, 87*(0), 65-76. doi: http://dx.doi.org/10.1016/j.atmosenv.2014.01.028

Van Loo, S., & Koppejan, J. (2010). *The handbook of biomass combustion and co-firing*. London ; Washington, DC: Earthscan.

Vassilev, S. V., Baxter, D., & Vassileva, C. G. (2013). An overview of the behaviour of biomass during combustion: Part I. Phase-mineral transformations of organic and inorganic matter. *Fuel, 112*(0), 391-449. doi: http://dx.doi.org/10.1016/j.fuel.2013.05.043

Williams, G. H. (1992). Fuel from Biomass. *Chemical & Engineering News, 70*(47), 3-3.